

A SPINNING CONSTRUCTION FOR VIRTUAL 1-KNOTS AND 2-KNOTS, AND THE FIBERWISE AND WELDED EQUIVALENCE OF VIRTUAL 1-KNOTS

LOUIS H. KAUFFMAN, EIJI OGASA, AND JONATHAN SCHNEIDER

ABSTRACT. Spun-knots (respectively, spinning tori) in S^4 made from classical 1-knots compose an important class of spherical 2-knots (respectively, embedded tori) contained in S^4 . Virtual 1-knots are generalizations of classical 1-knots. We generalize these constructions to the virtual 1-knot case by using what we call, in this paper, the spinning construction of a submanifold. The construction proceeds as follows: It has been known that there is a consistent way to make an embedded circle C contained in $(\text{a closed oriented surface } F) \times (\text{a closed interval } [0, 1])$ from any virtual 1-knot K . Embed F in S^4 by an embedding map f . Let F also denote $f(F)$. We can regard the tubular neighborhood of F in S^4 as $F \times D^2$. Let $[0, 1]$ be a radius of D^2 . We can regard $F \times D^2$ as the result of rotating $F \times [0, 1]$ around $F \times \{0\}$. Assume $C \cap (F \times \{0\}) = \emptyset$. Rotate C together when we rotate $F \times [0, 1]$ around $F \times \{0\}$. Thus we obtain an embedded torus $Q \subset S^4$. We prove the following: The embedding type Q in S^4 depends only on K , and does not depend on f . Furthermore, the submanifolds, Q and the embedded torus made from K , defined by Satoh's method, of S^4 are isotopic.

We generalize this construction in the virtual 1-knot case, and we also succeed to make a consistent construction of one-dimensional-higher tubes from any virtual 2-dimensional knot. Note that Satoh's method says nothing about the virtual 2-knot case. Rourke's interpretation of Satoh's method is that one puts 'fiber-circles' on each point of each virtual 1-knot diagram. If there is no virtual branch point in a virtual 2-knot diagram, our way gives such fiber-circles to each point of the virtual 2-knot diagram. Furthermore we prove the following: If a virtual 2-knot diagram α has a virtual branch point, α cannot be covered by such fiber-circles.

We obtain a new equivalence relation, the \mathcal{E} -equivalence relation of the set of virtual 2-knot diagrams, that is much connected with the welded equivalence relation and our spinning construction. We prove that there are virtual 2-knot diagrams, J and K , that are virtually nonequivalent but are \mathcal{E} -equivalent.

Although Rourke claimed that two virtual 1-knot diagrams α and β are fiberwise equivalent if and only if α and β are welded equivalent, we state that this claim is wrong. We prove that two virtual 1-knot diagrams α and β are fiberwise equivalent if and only if α and β are rotational welded equivalent (the definition of rotational welded equivalence is given in the body of the paper).

CONTENTS

1. Introduction	2
1.1. Spinning tori	2
1.2. History of relations between virtual knots and QFT, and a reason why virtual knots are important	2
1.3. Main results	6
2. $\mathcal{K}(K)$ for a virtual 1-knot K	8
3. $\mathcal{E}(K)$ for a virtual 1-knot K	10
4. Proof of Theorems 3.3 and 3.4	13
5. Immersed solid tori	20
6. The virtual 2-knot case	21
7. The \mathcal{E} -equivalence	44
8. The fibrewise equivalence	47
8.1. The fibrewise equivalence is equal to the rotational welded equivalence, and is different from the welded equivalence of virtual 1-knots	47
8.2. Related topics	76
9. Virtual high dimensional knots	82
References	84

1. INTRODUCTION

1.1. Spinning tori.

Spun-knots (respectively, spinning tori) in S^4 made from classical 1-knots compose an important class of spherical 2-knots (respectively, embedded tori) contained in S^4 . See [45] for the definition of spun-knots. We review the construction of them below.

Let $\mathbb{R}^4 = \{(x, y, z, w) | x, y, z, w \in \mathbb{R}\}$. Regard \mathbb{R}^4 as the result of rotating $H = \{(x, y, z, w) | x \geq 0, w = 0\}$ around $A = \{(x, y, z, w) | x = 0, w = 0\}$ as the axis. Take a 1-knot K in H so that $K \cap A$ is an arc (respectively, the empty set). Rotate $K - \text{Int}(K \cap A)$ around A together when we rotate H around A . The resultant submanifold of \mathbb{R}^4 is the spun knot (respectively, the spinning tori) of K . We can easily also regard them as submanifolds of S^4 . We can define a spun link if K is a link although we discuss the knot case mainly in this paper. Our discussion can be easily generalized to the link case.

One of our themes in this paper is to generalize the spun knots of classical knots to the virtual knot case. We begin by explaining why virtual knots are important.

1.2. History of relations between virtual knots and QFT, and a reason why virtual knots are important.

Virtual 1-links are defined in [15, 16, 17] as generalizations of classical 1-links. One motivation for virtual 1-links is as follows. Jones [11] defined the Jones polynomial for classical 1-links in S^3 . The following had been well-known before the Jones polynomial was found: The Alexander polynomial for classical 1-links in S^3 is defined in terms of the topology of the complement of the link and can be generalized to give invariants of closed oriented 3-manifolds and of links within the 3-manifold.

Jones [11, page 360, §10] tried to define a 3-manifold invariant associated with the Jones polynomial, and succeeded in some cases. Of course, when the Jones polynomial was found, the following question was regarded as a very natural one:

Question J. Can we generalize the definition of the Jones polynomial for classical 1-links in S^3 to that in any 3-manifold?

Note the result may not be a polynomial but a function of t .

Witten [44] wrote a quantum field theoretic path integral for any 1-link L in any compact oriented 3-manifold M . His path integral included the Jones polynomial for 1-links in S^3 , its generalizations and new (at the time) invariants of 3-manifolds. This was a breakthrough for the philosophy of physics in that one of the most natural geometrically intrinsic interpretations of a mathematical object was done by using a path integral, and had not been done by any other way.

Note. Here, ‘geometrically intrinsic interpretation’ means the point of view that would define a link invariant in terms of the embedding of the link in the ambient 3-dimensional manifolds just as one can do naturally and easily in the case of the Alexander polynomial of 1-knots. Jones [11] defined the Jones polynomial by using representations of braid groups to an operator algebra (the Temperley-Lieb algebra). Representations, braid groups, operator algebras are mathematically explicit objects so some people may feel that that is enough to consider the meaning of the Jones polynomial.

If $M = S^3$, we can say at the physics level that the Witten path integral represents the Jones polynomial for 1-links in S^3 . Reshetikhin, Turaev, Lickorish and others [24, 29, 30, 36] etc. generalized the result in [11, page 360, §10] and created rigorous definitions for invariants of 3-manifolds that parallel Witten’s ideas, without using the functional integral. They succeeded to define new invariants of closed oriented 3-manifolds and invariants of links embedded in 3-manifolds that we today call quantum invariants. (Note, here, we distinguish the above invariants of links embedded in 3-manifolds with the Jones polynomial for them as below.) In both Witten’s version and the Reshetikhin-Turaev versions the invariants of 3-manifolds are obtained by representing the 3-manifold as surgery on a framed link and summing over invariants corresponding to appropriate

representations decorating the surgery link. The same technique applies when one includes an extra link component that is not part of the surgery data. In this way, one obtains quantum invariants of links in 3-manifolds. Another technique, formalized by Crane [5] and by Kohno [25] uses a Heegard decomposition of the 3-manifold and algebraic structure of the conformal field theory for the surface of the Heegard decomposition. These methods produce invariants for 3-manifolds and, in principle, invariants for links in 3-manifolds, but are much more indirect than the original physical idea of Witten that would integrate directly over the many possible evaluations of the Wilson loop for the knot or link in the 3-sphere, or the original combinatorial skein techniques that produce the invariant of a link from its diagrammatic combinatorics. See [14].

The Witten path integral is written also in the case where $L \neq \phi$ and $M \neq S^3$. It corresponded to Question J, which had been considered before the Witten path integral appeared.

In [12] Kauffman found a definition of the Jones polynomial as a state summation over combinatorial states of the link diagram and found a diagrammatic interpretation of the Temperley-Lieb algebra that put the original definition of Jones in a wider context of generalized partition functions and statistical mechanics on graphs and knot and link diagrams. In [15, 16, 17] Kauffman generalized the Jones polynomial in the case where M is $(\text{a closed oriented surface}) \times [-1, 1]$. In fact, [15, 16, 17] defined virtual 1-links as another way of describing 1-links in $(\text{a closed oriented surface}) \times [-1, 1]$: the set of virtual 1-links is the same as that of 1-links in $(\text{a closed oriented surface}) \times [-1, 1]$, taken up to handle stabilization. See Theorem 2.1. We make the point here that the virtual knot theory is a context for links in the fundamental 3-manifolds of the form $F \times I$ where F is a closed surface. The state summation approach to the Jones polynomial generalizes to invariants of links in such thickened surfaces. This provides a significant and direct arena for examining such structures without the functional integral. It also provides challenges for corresponding approaches that use the functional integral methods. It remains a serious challenge to produce ways to work with the functional integrals that avoid difficulties in analysis.

Path integrals represent the superposition principle dramatically. This is a marvelous idea of Feynman. The Witten path integral also represents a geometric idea of the Jones polynomial and quantum invariants physics-philosophically very well. Witten found a Lagrangian via the Chern-Simons 3-form and Wilson line with a tremendous insight, and he calculated the path integral of the Lagrangian rigorously at physics level, and showed that the result of the calculation is the Jones polynomial for links in S^3 , and the quantum invariants of any closed oriented 3-manifold with or without embedded circles. It is a wonderful work of Witten. However recall the following facts: The Witten path

integral for any 1-link in any closed 3-manifold has not been calculated in mathematical level nor in physics level in any way that can be regarded as direct. This means that Question J is open in the general case. That is, nobody has succeeded to generalize the Jones polynomial in a direct way, and mathematically rigorously to the case where M is not S^3 , (respectively, B^3, \mathbb{R}^3), nor $(\text{a closed oriented surface } F) \times [-1, 1]$. (Note the last manifold is not closed. Note that the discussion in the S^3 case is the same as that in the B^3 (respectively, \mathbb{R}^3) case. Virtual knot theory can also discuss the case where F is compact and non-closed, but then we need to fix the embedding type of F in $F \times [-1, 1]$.)

Recall the following fact: Even if we make a (seemingly) meaningful Lagrangian, the path integral associated with the Lagrangian cannot always be calculated. An example is the Witten path integral associated with the general case of Question J. Another one is the following. Today they do not know how to calculate the path integral if we replace Chern-Simons-3-form on 3-manifolds with Cern-Simons- $(2p+1)$ -form on $(2p+1)$ -manifolds, where p is any integer ≥ 2 , in the Witten path integral. Indeed nowadays they only calculate path integrals only when they can calculate them. If the path integral of the Lagrangian is not calculated explicitly, neither mathematicians nor physicists regard the theory of the Lagrangian as a meaningful one. Furthermore, even if we calculate path integrals, the result of the calculation is sometimes what we do not expect. See an example of [26] explained in [39, the last part of section 5.1].

The heuristics of the Witten path integral have not been fully mined. See [19] for a survey of the results of some of these heuristics in relation to the Jones polynomial and Vassiliev invariants. It is possible that good heuristics will emerge for understanding invariants of links in 3-manifolds. But at the present time it is worth examining the cases we do understand for working with generalizations of the Jones polynomial for links in thickened surfaces. We had begun considering Question J before the Witten path integral appeared in this discussion. Question J is also natural and important even if we do not consider path integrals.

Note. (1) We can observe some historical correspondences. Feynman discovered path integrals by using an analogy with (quantum) statistical mechanics, and he interpreted quantum theory by using path integrals. Operator algebras, path integrals, (quantum) statistical mechanics are closely related. The Jones polynomial is discovered by using operator algebras ([11]), next is interpreted via (quantum) statistical mechanics ([12]), then by using path integrals ([44]). Operator algebras, path integrals, and (quantum) statistical mechanics are related again with topology in the background.

(2) The Jones polynomial of 1-links in $(\text{a closed oriented surface}) \times (\text{the interval})$ is discovered in [15, 16, 17], by using the analogy with state sums in (quantum) statistical mechanics in [12].

(3) [13] found a relation between the Alexander-Conway polynomial between 1-dimensional classical knots and quantum field theory. The relation gives a different aspect from the Homflypt polynomial and the Witten path integral. [33] found a relation between the degree of the Alexander polynomial of high dimensional knots and the Witten index of a supersymmetric quantum system. It is also an outstanding open question whether we can define an analog to the Jones polynomial for high dimensional knots.

Virtual 1-links have many other important properties than the above one. See [15, 16, 17]. Thus it is very natural to consider whether any property of classical 1-knots is possessed by virtual 1-knots, as below.

1.3. Main results.

We generalize the construction of spun-knots (respectively, spinning tori) of classical 1-knots to the virtual 1-knot case as follows. Recall that, in [15, 16, 17] there is given a consistent way to make an embedded circle C contained in $(\text{a closed oriented surface } F) \times (\text{a closed interval } [0, 1])$ from any virtual 1-knot K diagram (see Theorem 2.1). Note the following. When we construct spun knots (spinning tori), we regard \mathbb{R}^4 itself as the total space of the normal bundle of A in \mathbb{R}^4 . Recall that A is defined in §1.1. Embed F in $\mathbb{R}^4 \subset S^4$ by an embedding map f . Let F stand for $f(F)$. Note that the tubular neighborhood of F in S^4 is diffeomorphic to $F \times D^2$. Let $[0, 1]$ be a radius of D^2 . We can regard $F \times D^2$ as the result of rotating $F \times [0, 1]$ around $F \times \{0\}$. Assume $C \cap (F \times \{0\}) = \phi$. Rotate C together when we rotate $F \times [0, 1]$ around $F \times \{0\}$. Thus we obtain an embedded torus $Q \subset S^4$.

We prove the following (Theorems 3.3 and 3.4): The embedding type Q in S^4 depends only on K , and does not depend on f . Furthermore the submanifolds, Q and the embedded torus made from K defined by Satoh in [40], of S^4 are isotopic.

This construction of Q is an example of what we call the spinning construction of submanifolds in Definition 3.1. This paper does not discuss the case where $C \cap (F \times \{0\}) \neq \phi$.

There are classical 1-knots, virtual 1-knots, and classical 2-knots so it is natural to consider virtual 2-knots. We define virtual 2-knots in Definition 6.3. It is very natural to consider whether any property of ‘classical 1-, and 2-knots and virtual 1-knots’ is possessed by virtual 2-knots. It is natural to ask whether we can define one-dimensional-higher tubes for virtual 2-knots (Question 6.4) since we succeed in the virtual 1-knot case

as explained above. Note that Satoh's method in [40] does not treat the virtual 2-knot case.

In the virtual 1-knot case, in [38], Rourke interpreted Satoh's method as follows: Let α be any virtual 1-knot diagram. Put 'fiber-circles' on each point of α and obtain a one-dimensional-higher tube. (We review this construction in Theorem 4.3 and Definition 4.4). If we try to generalize Rourke's way to the virtual 2-knot case, we encounter the following situation.

Let α be any virtual 1-knot diagram. There are two cases:

- (1) The case where α has no virtual branch point. (We define virtual branch point in Definitions 6.1 and 6.3.)
- (2) The case where α has a virtual branch point.

In the case (1), we can make a tube by Rourke's method. See [41, section 3.7.1], Note 6.5, and Definition 6.6. In the case (2), however, Schneider [41] found it difficult to define a tube near any virtual branch point.

Thus we consider the following two problems.

Can we put fiber-circles over each point of any virtual 2-knot in a consistent way as described above, and make a one-dimensional-higher tube (Question 6.7)?

Is there a one-dimensional-higher tube construction which is defined for all virtual 2-knots, and which agrees with the method in the case (1) written above when there are no virtual branch points (Question 6.8)?

In Theorem 6.16 we give an affirmative answer to Question 6.8. Our solution is a generalization of our method in the virtual 1-knot case used in §§3-4. We also use a spinning construction of submanifolds explained in Definition 3.1.

In Theorem 6.23 we give a negative answer to Question 6.7.

We obtain a new equivalence relation, the \mathcal{E} -equivalence relation of the set of virtual 1- and 2-knot diagrams (Definition 7.1). It is done by using the above spinning construction. The \mathcal{E} -equivalence relation is closely connected with the welded equivalence relation and our spinning construction. Welded 1-links are defined in [38] associated with virtual 1-links. Welded 1-links are related to tubes very much as we discuss in this paper. We

introduce welded 2-knots in Definition 8.15.

We prove that there are virtual 2-knot diagrams, J and K , that are virtually nonequivalent but are \mathcal{E} -equivalent (Theorem 7.6). Welded 1-, and 2-knots are recipients of the tube construction or the above spinning construction. The above spinning construction is related to the fiberwise equivalence explained below. We will explain their connection in this paper and this is a theme of this research.

Although Rourke claimed in [38, Theorem 4.1] that two virtual 1-knot diagrams α and β are fiberwise equivalent if and only if α and β are welded equivalent, we state that this claim is wrong. (See [38] and Definitions 8.1 of this paper for the definition of the fiberwise equivalence, and [38, 40] for that of the welded equivalence.) The reason for the failure of Rourke's claim is given in Theorems 8.5 and 8.39, and Claim 8.47. We prove in Theorems 8.5 and 8.39 that *virtual 1-knot diagrams, α and β , are fiberwise equivalent if and only if they are rotational welded equivalent*. The reader can recall that in virtual 1-knot theory there are Reidemeister-type moves for virtual crossings. Rotational equivalence for virtual knots is obtained by making the virtual curl (analog of the first Reidemeister move) forbidden. Rotational equivalence for welded knots also forbids the virtual curl move in the context of the rules for welded knots. (See [16, 18, 41] for rotational welded equivalence.) Our result is proved by using the property of virtual 2-knots found in Theorem 6.23. Virtual 2-knots themselves are important, and furthermore they are also important for research in virtual 1-knots. Our main results are Theorems 3.3, 3.4, 6.16, 6.23, 7.6, 8.5, and 8.48.

2. $\mathcal{K}(K)$ FOR A VIRTUAL 1-KNOT K

We work in the smooth category unless we indicate otherwise. In a part of §8 we will use the PL category in order to prove our results in the smooth category. See Note 8.9. We review some facts on virtual 1-knots in this section before we state two of our main results, Theorems 3.3 and 3.4, in the following section.

Let α be a virtual 1-knot diagram. In this paper we use Greek lowercase letters for virtual diagrams and Roman capital letters for virtual knots. See [15, 16, 17] for the definition and properties of virtual 1-knot diagrams and those of virtual 1-knots. For α there are a nonnegative integer g and an embedded circle contained in $\Sigma_g \times [0, 1]$ as follows, where Σ_g is a closed oriented surface with genus g . Take α in \mathbb{R}^2 . (Recall that we can make the infinity point $\{*\}$ and \mathbb{R}^2 into S^2 .) Carry out a surgery on \mathbb{R}^2 by using a 3-dimensional 1-handle near a virtual crossing point as shown in Figure 2.1 and obtain

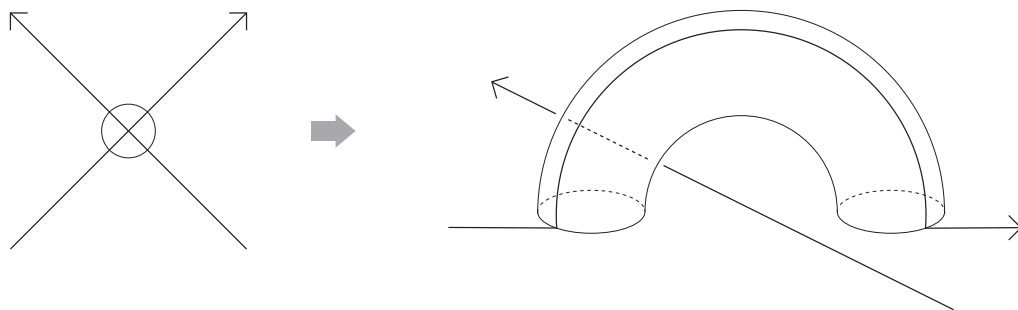


FIGURE 2.1. **A virtual crossing point and a surgery by a 1-handle**

$T^2 - \{*\}$. Note that the virtual 1-knot K is oriented and that the arrows in Figure 2.1 denote the orientation. Segments are changed as shown in the right figure of Figure 2.1. Do this procedure near all virtual crossing points. Suppose that α has g copies of virtual crossing point ($g \in \mathbb{N} \cup \{0\}$). Here, \mathbb{N} denotes the set of natural numbers. Note that a is a natural number if and only if a is a positive integer. What we obtain is $\Sigma_g - \{*\}$. We call it Σ_g^\bullet . (In §4, for a closed oriented surface F , we define F° to be $F -$ (an open 2-disc).

So, here, we use \bullet not \circ .) Thus we obtain an immersed circle in Σ_g^\bullet from α . Call it $\mathcal{I}(\alpha)$. Note that it is an immersion in ordinary sense (that is, it has no ‘virtual crossing point’). Regard Σ_g as an abstract manifold. Make $\Sigma_g^\bullet \times [0, 1]$. There is a naturally embedded circle $\mathcal{L}(\alpha)$ contained in $\Sigma_g^\bullet \times [0, 1]$ whose projection by the projection $\Sigma_g^\bullet \times [0, 1] \rightarrow \Sigma_g^\bullet \times \{0\}$ is $\mathcal{I}(\alpha)$. Suppose that $\mathcal{L}(\alpha) \cap (\Sigma_g^\bullet \times \{0\}) = \phi$. Let $\mathcal{K}(\alpha)$ be an embedded circle in $\Sigma_g \times [0, 1]$ which we obtain naturally from $\mathcal{L}(\alpha)$. Σ_g is called a *representing surface*. $\Sigma_g^\bullet = \Sigma_g - \{*\}$ is also sometimes called a *representing surface*. (The closure of) any neighborhood of the immersed circle in Σ_g is also called a *representing surface*.

Theorem 2.1. ([15, 16, 17].) *Let α and β be virtual 1-knot diagrams. α and β represent the same virtual 1-knot if and only if $\mathcal{K}(\alpha)$ is obtained from $\mathcal{K}(\beta)$ by a sequence of the following operations.*

- (1) *A surgery on the surface by a 3-dimensional 1-handle, where
(The attached part of the handle) \cap (the projection of the embedded circle) $= \phi$.*
- (2) *A surgery on the surface by a 3-dimensional 2-handle, where
(The attached part of the handle) \cap (the projection of the embedded circle) $= \phi$.*
- (3) *An orientation preserving diffeomorphism map of the surface.*

Hence the following definition makes sense. Let K be a virtual 1-knot. Let α be a virtual 1-knot diagram of K . Define $\mathcal{K}(K)$ to be $\mathcal{K}(\alpha)$.

3. $\mathcal{E}(K)$ FOR A VIRTUAL 1-KNOT K

We generalize spun knots and spinning tori, and introduce a new class of submanifolds.

Let n be a positive integer. Two submanifolds J and $K \subset S^n$ are (*ambient*) *isotopic* if there is a smooth orientation preserving family of diffeomorphisms η_t of S^n , $0 \leq t \leq 1$, with η_0 the identity and $\eta_1(J) = K$.

Definition 3.1. Let F be a codimension two submanifold contained in a manifold X . Suppose that the tubular neighborhood $N(F)$ of F in X is the product bundle. That is, we can regard $N(F)$ as $F \times D^2$. See Figure 3.1. We can regard the closed 2-disc D^2 as the result of rotating a radius $[0, 1]$ around the center $\{o\}$ as the axis. We can regard $N(F)$ as the result of rotating $F \times [0, 1]$ around $F = F \times \{0\}$ as the axis. Suppose that a submanifold P contained in X is embedded in $F \times [0, 1]$. Let P' be a submanifold $P \cap (F \times \{0\})$ of $F \times \{0\}$. When we rotate $F \times [0, 1]$ around F and make $F \times D^2$, rotate P together, and call the resultant submanifold Q . This submanifold Q contained in X is called the *spinning submanifold* made from P by the rotation in $F \times D^2$ under the

condition that $P \cap (F \times \{0\})$ is the submanifold P' . This way of construction of Q is called a *spinning construction* of submanifolds. If P is a subset not a submanifold, we can define Q as well.

Spun knots and spinning tori are spinning submanifolds. [31, Proof of Claim in page 3114] and [32, Lemma 5.3] used spinning construction. By the uniqueness of the tubular neighborhood, we have the following.

Claim 3.2. *Let \check{f} (respectively, \check{g}) : $F \times D^2 \hookrightarrow X$ be an embedding map. We can regard $\check{f}(\Sigma_g \times D^2)$ (respectively, $\check{g}(\Sigma_g \times D^2)$) as the tubular neighborhood of $\check{f}(\Sigma_g \times \{o\})$ (respectively, $\check{g}(\Sigma_g \times \{o\})$). Let $\check{f}|_{\Sigma_g \times \{o\}}$ be isotopic to $\check{g}|_{\Sigma_g \times \{o\}}$. Then submanifolds, $\check{f}(\Sigma_g \times \{o\})$ and $\check{g}(\Sigma_g \times \{o\})$, of X are isotopic.*

Let α be a virtual 1-knot diagram. Take $\Sigma_g \times [0, 1]$ and $\mathcal{K}(\alpha)$ as in §2, that is, $K(\alpha)$ is a 1-knot in $\Sigma_g \times [0, 1]$, where Σ_g representing α . Assume $\mathcal{K}(\alpha) \cap (\Sigma_g \times \{0\}) = \emptyset$. Suppose $\mathcal{K}(\alpha) \cap (\Sigma_g \times \{1\}) = \emptyset$. Make $\Sigma_g \times D^2$, where we regard $[0, 1]$ as a radius of D^2 . Let $\check{f} : \Sigma_g \times D^2 \hookrightarrow S^4$ be an embedding map. Let $\mathcal{E}_{\check{f}}(\alpha)$ be the spinning submanifold made from $\mathcal{K}(\alpha)$ by the rotation in $\check{f}(\Sigma_g \times D^2)$. Note $\mathcal{E}_{\check{f}}(\alpha) \subset S^4$. Let f be $\check{f}|_{\Sigma_g \times \{o\}}$. By Claim 3.2 it makes sense that we call $\mathcal{E}_{\check{f}}(\alpha)$, $\mathcal{E}_f(\alpha)$.

Suppose that α represents a virtual 1-knot K . Theorem 3.3 is one of our main results.

Theorem 3.3. *For an arbitrary virtual 1-knot K , the submanifold type $\mathcal{E}_f(\alpha)$ of S^4 does not depend on the choice of a set (α, f) .*

By Theorem 3.3 we can define $\mathcal{E}(K)$ for any virtual 1-knot K .

Let $\mathcal{S}(\alpha)$ be an embedded $S^1 \times S^1$ contained in S^4 for a virtual 1-knot diagram α , defined by Satoh in [40]. It was proved there that if α and β represent the same virtual 1-knot, the submanifolds, $\mathcal{S}(\alpha)$ and $\mathcal{S}(\beta)$, of S^4 are isotopic. So we can define $\mathcal{S}(K)$ for any virtual 1-knot K .

We will prove the following in §4.

Theorem 3.4 is one of our main results.

Theorem 3.4. *Let K be a virtual 1-knot. Then the submanifolds, $\mathcal{E}(K)$ and $\mathcal{S}(K)$, of S^4 are isotopic.*

Note 3.5. If K in Theorem 3.4 is a classical knot, $\mathcal{E}(K)$ and $\mathcal{S}(K)$ is the spinning torus of K .

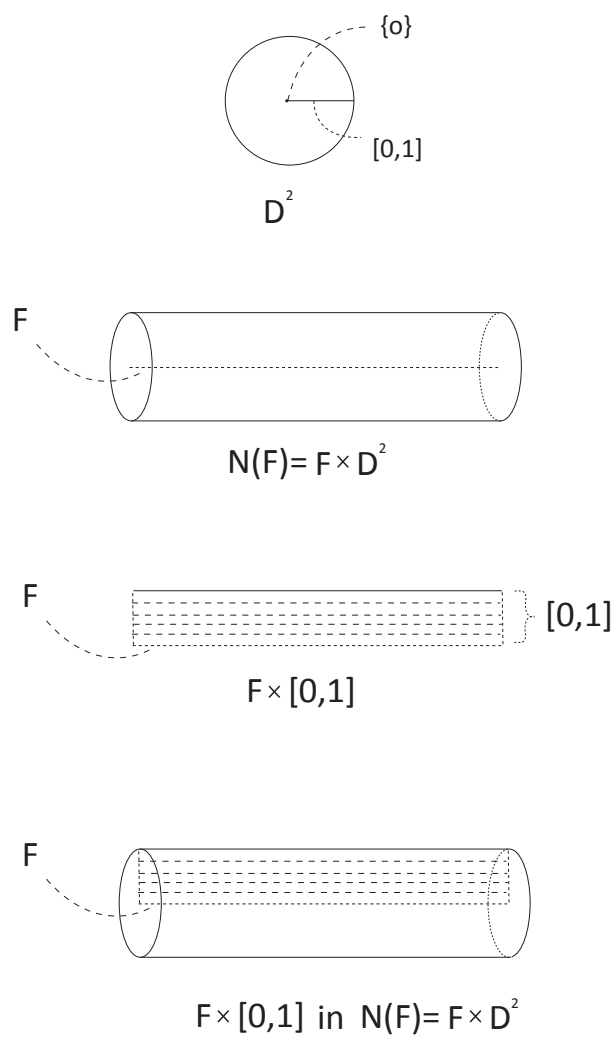


FIGURE 3.1. The tubular neighborhood which is a product D^2 -bundle

Note. [1, section 10.2], [2, section 3.1.1] and [43] proved only a special case of Theorem 3.4, which is only Theorem 4.1 of this paper. We prove the general case. Our result is stronger than the result in [1, section 10.2], [2, section 3.1.1] and [43].

4. PROOF OF THEOREMS 3.3 AND 3.4

We first prove a special case.

Theorem 4.1. *Take a virtual 1-knot diagram α in §2. Let $\tilde{\iota} : \Sigma_g \times D^2 \rightarrow S^4$ be an embedding map whose image of Σ_g^\bullet by $\tilde{\iota}$ is Σ_g^\bullet in §2. Let ι be $\tilde{\iota}|_{\Sigma_g}$. Then the submanifolds, $\mathcal{E}_\iota(\alpha)$ and $\mathcal{S}(\alpha)$, of S^4 are isotopic.*

Proof of Theorem 4.1. Let $\mathbb{R}^4 = \{(x, y, u, v) | x, y, u, v \in \mathbb{R}\}$, $\mathbb{R}_b^2 = \{(x, y) | x, y \in \mathbb{R}\}$, and $\mathbb{R}_F^2 = \{(u, v) | u, v \in \mathbb{R}\}$. Note $\mathbb{R}^4 = \mathbb{R}_b^2 \times \mathbb{R}_F^2$. Regard \mathbb{R}^3 in §2 as $\mathbb{R}_b^2 \times \{(u, v) | u \in \mathbb{R}, v = 0\}$. Take the tubular neighborhood of Σ_g^\bullet in \mathbb{R}^3 . It is diffeomorphic to $\Sigma_g^\bullet \times [-1, 1]$. We can suppose that $\Sigma_g^\bullet, \Sigma_g^\bullet \times [0, 1] \subset \mathbb{R}_b^2 \times \{(u, v) | u \geq 0, v = 0\}$.

Note. Let $\Sigma_g \subset S^4$. Suppose that $\{*\} \in S^4$ is included in Σ_g . Then $S^4 - \Sigma_g = (S^4 - \{*\}) - (\Sigma_g - \{*\}) = R^4 - \Sigma_g^\bullet$.

Take the tubular neighborhood $N(\Sigma_g^\bullet)$ of Σ_g^\bullet in \mathbb{R}^4 . Note that $N(\Sigma_g^\bullet)$ is diffeomorphic to $\Sigma_g^\bullet \times D^2$. We can regard $N(\Sigma_g^\bullet)$ as the result of rotating $\Sigma_g^\bullet \times [0, 1]$ around Σ_g^\bullet as the axis (diffeomorphically not isometrically). Suppose that $\mathcal{L}(\alpha) \cap (\Sigma_g^\bullet \times \{0\}) = \phi$. Make the spinning submanifold $\mathcal{E}_\iota(\alpha)$ from $\mathcal{L}(\alpha)$.

We can suppose that each fiber D^2 of $N(\Sigma_g^\bullet)$ is parallel to $\{(x, y) | x = 0, y = 0\} \times \mathbb{R}_F^2$ by using an isotopy of an embedding map of the tubular neighborhood.

We can suppose that $\mathcal{I}(\alpha)$ intersects each fiber D^2 transversely. *Reason.* Note a 1-handle drawn in the right-side of Figure 2.1. If $\mathcal{I}(\alpha)$ near the 1-handle is put like (Ac) in Figure 4.1, $\mathcal{I}(\alpha)$ does not intersect each fiber D^2 transversely. However we can do the following operation. By using an isotopy of a part of \mathcal{I} we change the part of $\mathcal{I}(\alpha)$ from (Ac) to (Ob) in Figure 4.1. After this operation, $\mathcal{I}(\alpha)$ intersects each fiber D^2 transversely.

Note 4.2. We will explain a property of (Ac), in Note 4.5. It is important. We will use it in Alternative proof of Claim 6.22 of §6.

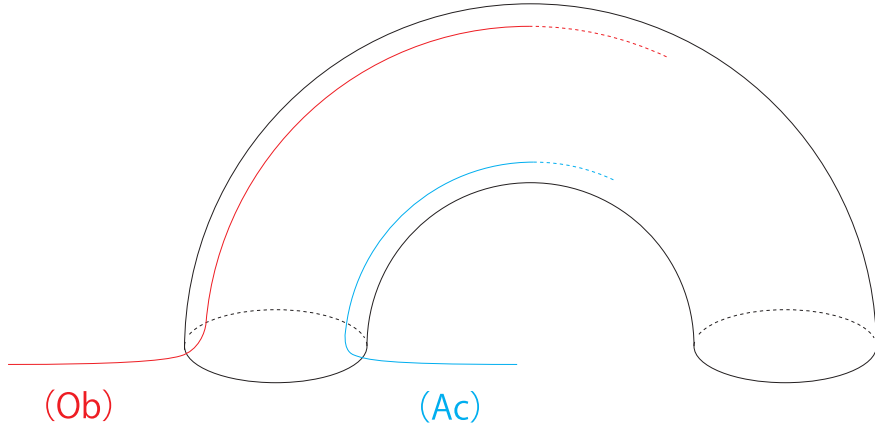


FIGURE 4.1. **(Ac)** and **(Ob)**.

Note that, even if a part of $\mathcal{I}(\alpha)$ is (Ac), we can make a spinning submanifold $\mathcal{E}_t(\alpha)$. However, if there is not (Ac), we have an advantage as below.

If there is not (Ac) in $\mathcal{I}(\alpha)$, we have the following.

Take a point $q \in \mathbb{R}_b^2 \times \{(u, v) | u = 0, v = 0\}$. Note $\alpha \subset \mathbb{R}_b^2 \times \{(u, v) | u = 0, v = 0\}$. By the above construction of $\mathcal{E}_t(\alpha)$, we have the following.

- (i) If $q \cap \alpha = \phi$, $(\{q\} \times \mathbb{R}_F^2) \cap \mathcal{E}_t(\alpha) = \phi$.

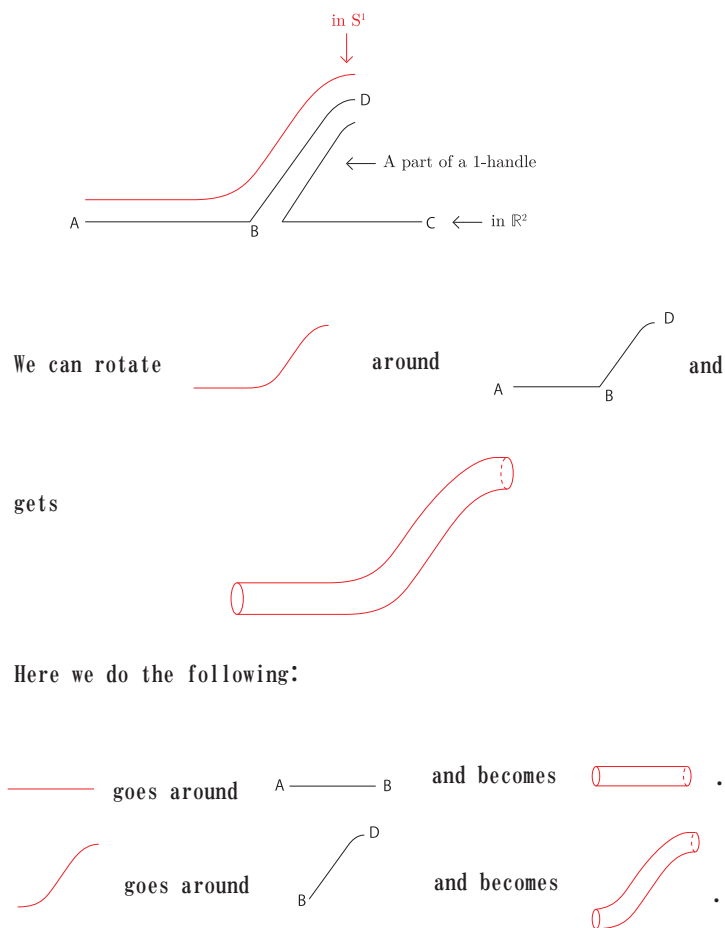


FIGURE 4.2. Rotation around a part near (Ob). The reason why (Ob) is useful for us.

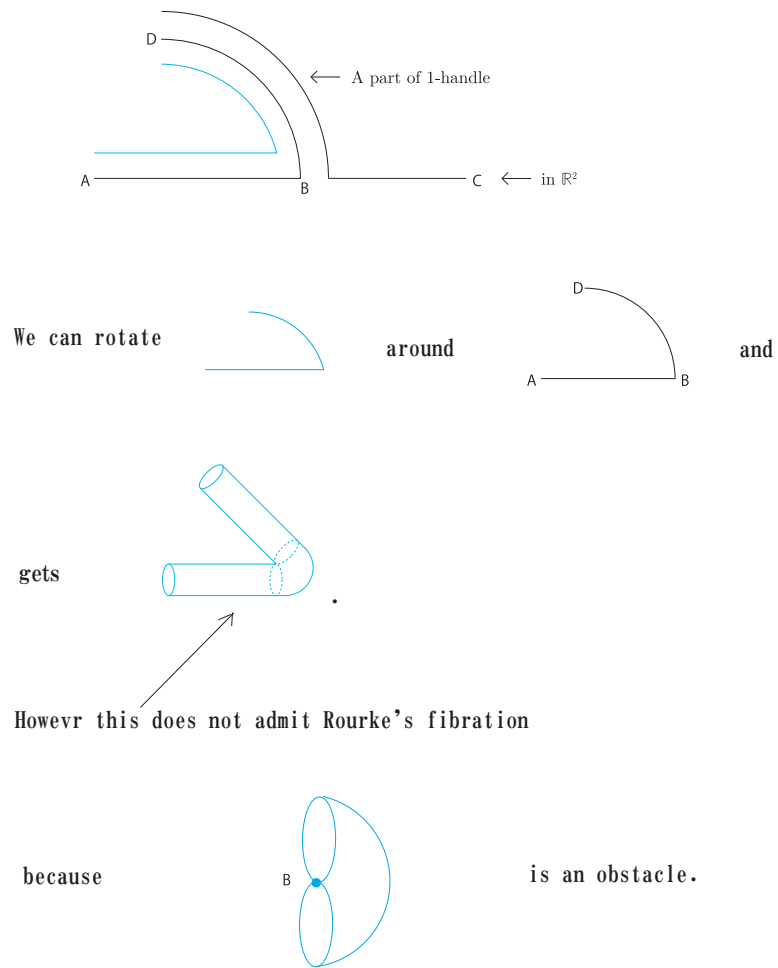


FIGURE 4.3. Rotation around a part near (Ac) . The reason why (Ac) is not useful for us. This property of (Ac) is used in in Alternative proof of Claim 6.22 of §6.

- (ii) If q is a normal point of α , $(\{q\} \times \mathbb{R}_F^2) \cap \mathcal{E}_i(\alpha)$ is a single circle in $\{q\} \times \mathbb{R}^2$.
- (iii) If q is a real crossing point of α , $(\{q\} \times \mathbb{R}_F^2) \cap \mathcal{E}_i(\alpha)$ is two circles in $\{q\} \times \mathbb{R}^2$ such that one of the two is in the inside of the other. The inner (respectively, outer) circle corresponds to the lower (respectively, upper) point of the singular point.
- (iv) If q is a virtual crossing point of α , $(\{q\} \times \mathbb{R}_F^2) \cap \mathcal{E}_i(\alpha)$ is two circles in $\{q\} \times \mathbb{R}^2$ such that each of the two is in the outside of the other each other.

It is Rourke's description of $\mathcal{S}(\alpha)$ in Theorem 4.3 which is cited below from [38]. (However [38] does not write a proof. So [41] wrote a proof.)

Theorem 4.3. ([38].) *Let α be a virtual 1-knot diagram. Take an embedding map $\varphi : S_b^1 \times S_f^1 \hookrightarrow \mathbb{R}_b^2 \times \mathbb{R}_f^2$ with the following properties.*

(1) *Let $\pi : \mathbb{R}_b^2 \times \mathbb{R}_f^2 \rightarrow \mathbb{R}_b^2$ be the natural projection. $\pi \circ \varphi(S_b^1 \times S_f^1) \subset \mathbb{R}_b^2$ defines α without the notations of virtual crossings.*

(2) *For points in \mathbb{R}_b^2 , we have the following:*

- (i) *If $q \notin \alpha$, we have $\pi^{-1}(q) = \emptyset$.*
- (ii) *If q is a normal point of α , we have that $\pi^{-1}(q)$ is a circle in $\{q\} \times \mathbb{R}^2$.*
- (iii) *If q is a real crossing point of α , we have that $\pi^{-1}(q)$ is two circles in $\{q\} \times \mathbb{R}^2$ such that one of the two is in the inside of the other. The inner (respectively, outer) circle corresponds to the lower (respectively, upper) point of the singular point.*
- (iv) *If q is a virtual crossing point of α , we have that $\pi^{-1}(q)$ is two circles in $\{q\} \times \mathbb{R}^2$ such that each of the two is in the outside of the other each other.*

Then the submanifolds, $\mathcal{S}(\alpha)$ and $\varphi(S_b^1 \times S_f^1)$, of S^4 are isotopic

This completes the proof of Theorem 4.1. □

Definition 4.4. In Theorem 4.3, each circle $f(S_b^1 \times S_f^1) \cap (\text{each fiber } \mathbb{R}_f^2)$ is called a *fiber-circle*. We say that $f(S_b^1 \times S_f^1)$ admits *Rourke's fibration*.

Note 4.5. As we preannounced in Note 4.2, we state a comment on (Ac). If the projection on a surface includes (Ac), $\mathcal{E}(\alpha)$ does not admit Rourke's fibration. The reason is explained in Figures 4.2 and 4.3. We will use this property, which is raised by the difference between (Ac) and (Ob), in Alternative proof of Claim 6.22 of §6.

We next prove the general case.

Proof of Theorems 3.3 and 3.4. We prove Theorem 4.7 below. The key idea of the proof is Claim 4.6. Let Σ be a closed oriented surface. Let G_1 and G_2 be submanifolds

of S^4 which are orientation preserving diffeomorphic to Σ . It is known that there is a case that the submanifolds, G_1 and G_2 , of S^4 are non-isotopic. Let Σ° denote $\Sigma -$ (an open 2-disc). Let

$$G_i^\circ = G_i - (\text{an open 2-disc})$$

be a submanifold of S^4 which are orientation preserving diffeomorphic to Σ° ($i = 1, 2$).

Claim 4.6. *The submanifolds, G_1° and G_2° , of S^4 are isotopic.*

Proof of Claim 4.6. Σ° has a handle decomposition which consists of one 0-handle, 1-handles, and no 2-handle. \square

Let $i \in \{1, 2\}$. We can regard the tubular neighborhood of G_i in S^4 as $G_i \times D^2$. Embed S^1 in $G_i \times [0, 1]$, where we regard $[0, 1]$ as a radius of D^2 , and call the image J_i . Assume that $J_i \cap (G_i \times \{0\}) = \phi$. Suppose that there is a bundle map $\tilde{\sigma} : G_1 \times D^2 \rightarrow G_2 \times D^2$ such that $\tilde{\sigma}$ covers an orientation preserving diffeomorphism map $\sigma : G_1 \rightarrow G_2$ and such that $\tilde{\sigma}(J_1) = J_2$.

Define a submanifold E_i contained in S^4 to be the spinning submanifold made from J_i by the rotation in $G_i \times D^2$.

Theorem 4.7. *The submanifolds, E_1 and E_2 , of S^4 are isotopic.*

Proof of Theorem 4.7. We can suppose that $J_i \subset G_i^\circ \times [0, 1]$. By the existence of σ , there is a bundle map $\tilde{\tau} : G_1^\circ \times D^2 \rightarrow G_2^\circ \times D^2$ such that $\tilde{\tau}$ covers an orientation preserving diffeomorphism map $\tau : G_1^\circ \rightarrow G_2^\circ$ and such that $\tilde{\tau}(J_1) = J_2$.

Note the following: Let $f : \Sigma^\circ \rightarrow S^4$ be an embedding map. We can regard τ as a diffeomorphism map $\Sigma^\circ \rightarrow \Sigma^\circ$. By Claim 4.6, the submanifolds, $f(\Sigma^\circ)$ and $f(\tau(\Sigma^\circ))$, of S^4 are isotopic. Therefore the submanifolds, E_1 and E_2 , of S^4 are isotopic, \square

Theorems 2.1 and 4.7 imply Theorems 3.3 and 3.4 \square

We can extend all discussions in §§2-4 and the following §5 to the virtual 1-link case easily. When we define $\mathcal{E}(\alpha)$ in §3, we assume $\mathcal{L}(\alpha) \cap \Sigma_g^\bullet = \phi$. Suppose that $\mathcal{L}(\alpha) \cap (\Sigma_g^\bullet)$ is an arc instead. Then we obtain a spherical 2-knot in \mathbb{R}^4 as the spinning submanifold. The class of such spherical 2-knots is also a generalization of 2-dimensional spun-knots of 1-knots, and is also worth studying. As we state in §1, we do not discuss this class in this paper.

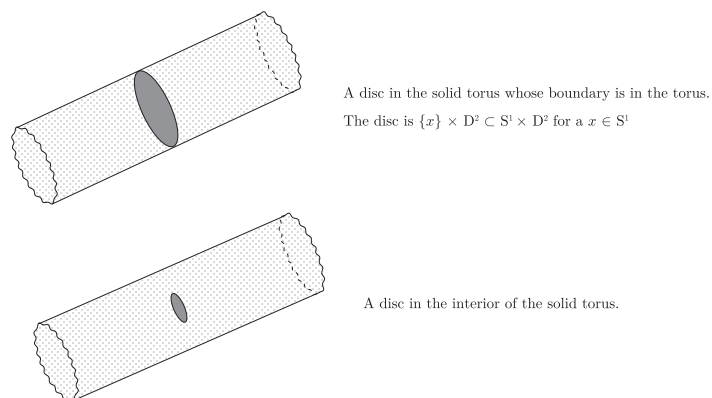


FIGURE 5.1. ζ^{-1} (each closed 2-disc)

5. IMMERSED SOLID TORI

By the definition of $\mathcal{S}(\cdot)$ in [40], we have (i) \Rightarrow (ii).

(i) An embedded torus Y contained in S^4 is isotopic to $\mathcal{S}(\alpha)$ for a virtual 1-knot diagram α .

(ii) There is an immersion map $\zeta : S^1 \times D^2 \looparrowright S^4$ with the following properties: $\zeta(S^1 \times \partial D^2)$ is Y . The singular point set of ζ consists of double points and is a disjoint union of closed 2-discs, and ζ^{-1} (each closed 2-disc) is as shown in Figure 5.1.

By using the construction of $\mathcal{E}(\alpha)$, we can also describe the immersed solid torus in (ii) as follows: By using the projection ' $\mathcal{L}(\alpha) \rightarrow \mathcal{I}(\alpha)$ ' in §2, we can make an immersed annulus in $\Sigma_g \times [0, 1]$ naturally. Note that $(\text{the immersed annulus}) \cap \Sigma_g \times \{0\} \neq \emptyset$. Make a subset from this immersed annulus by a spinning construction around Σ_g , defined in Definition 3.1. Then the result is an immersed solid torus in (ii).

We prove the converse of the above claim, that is, the following.

Theorem 5.1. (ii) \Rightarrow (i).

We prove this theorem as an application of our results in §4 although it may be also proved in another way.

Proof of Theorem 5.1. Let $q \in \partial D^2$. Let C be $\zeta(S^1 \times \{q\})$. In the following paragraphs, for Y , we will make an embedded oriented surface F contained in S^4 so that we will put C in the tubular neighborhood $N(F)$ of F in S^4 . We will make $C \cap F = \emptyset$. We will make Y so that it will be the spinning submanifold of C around F . Let $\{o\}$ be the center of D^2 . We will let F include $\zeta(S^1 \times \{o\})$.

Let $\xi : S^1 \times D^2 \times I \looparrowright S^4$ be an immersion map, where $I = [-1, 1]$, to satisfy that $\xi|_{S^1 \times D^2 \times \{0\}} = \zeta$ and that

$$\xi(\{x\} \times \{o\} \times I) \perp \xi(\{x\} \times D^2 \times \{0\})$$

for each x if we give appropriate metrics to S^4 and $S^1 \times D^2 \times I$. Then we can suppose the following:

(1) $P = \xi(S^1 \times \{o\} \times I)$ is a boundary-connected-sum of n copies of the annulus ($n \in \mathbb{N}$).

See Figure 5.2 for an example of P .

(2) $Q = \xi(S^1 \times D^2 \times I)$ is a boundary-connected-sum of m -copies of $S^1 \times B^3$ ($m \in \mathbb{N}$).

(3) $\partial P \subset \partial Q$.

(4) Q is the tubular neighborhood of P in S^4 . Q is diffeomorphic to $P \times D^2$.

By the Mayer-Vietoris sequence, $H_1(S^4, Q; \mathbb{Z}) \cong H_1(S^4 - \text{Int}Q, \partial Q; \mathbb{Z}) \cong 0$. Hence there is an embedded oriented compact surface-with-boundary G contained in $S^4 - \text{Int}Q$ such that $\partial G = \partial P$ and that $G \cup P$ is an oriented closed surface F . (*Reason:* Consider

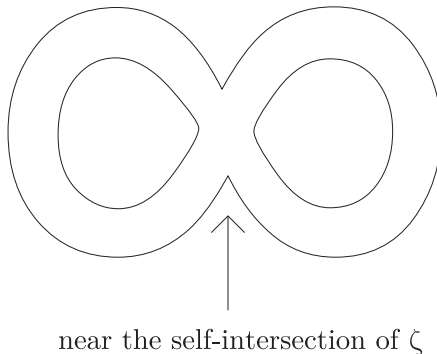


FIGURE 5.2. An example of P

a simplicial decomposition of $S^4 - \text{Int}Q$.) We can regard Y as the spinning submanifold made from $\zeta(S^1 \times \{q\})$ around F . Hence we can regard $\zeta(S^1 \times \{q\})$ as $\mathcal{K}(\beta)$ for a virtual 1-knot diagram β in a fashion which is explained in §§3-4, and can regard Y as $\mathcal{E}(\beta)$.

This completes the proof of Theorem 5.1. □

6. THE VIRTUAL 2-KNOT CASE

Virtual 2-knot theory is defined analogously to Virtual 1-knot theory, using generic surfaces in 3-space as knot diagrams and using Roseman moves for knot equivalence, and allowing the double-point arcs to have classical or virtual crossing data. See [42, 41]. Virtual 2-knot diagrams (respectively, virtual 2-knots) in [41] and this paper are the same as virtual surface-knots (respectively, virtual surface-knot diagrams) in [42].

Definition 6.1. Let F be a closed surface. A smooth map $f : F \rightarrow \mathbb{R}^3$ is considered *quasi-generic* if it fails to be one-to-one only at transverse crossings of orders 2 and 3 as shown in Figures 6.1 and 6.2, and it fails to be regular only at isolated *branch points* where, locally, the image of a disk looks like the cone over a loop, with no other parts of the surface touching the vertex. See Figure 6.3. Branch points include the cone over any closed, regular, transversely self-intersecting curve. In particular, the cone over a

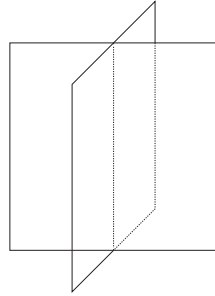


FIGURE 6.1. **Transversal double points**

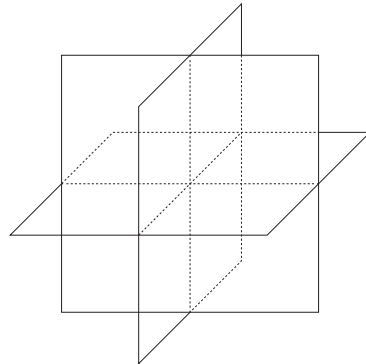


FIGURE 6.2. **Transversal triple points**

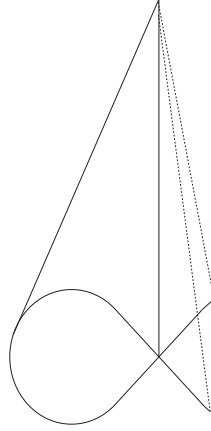


FIGURE 6.3. A general branch point

figure- ∞ curve is called a *Whitney branch point*. See Figure 6.4.

A quasi-generic map f is *generic* if the only branch points are Whitney branch points. The three features of a generic map— Whitney branch points, double-point arcs, and triple points— have slice-histories corresponding respectively to the Reidemeister *I*-, *II*-, and *III*- moves in 1-knot theory.

Definition 6.2. A *virtual 2-knot diagram* consists of a generic map F together with classical and virtual crossing data along its double-point arcs. Crossing data is represented graphically as broken and unbroken surfaces: See the left two figures of Figure 6.5. Branch points can be classical or virtual: See the middle three figures, the figures which are not the above ones nor the following ones, in Figure 6.5. At triple points, three crossings meet. Triple points of the following types are allowed: See the right three figures in Figure 6.5. All other combinations of crossing data are forbidden. Note that the three allowed triple points have slice-histories corresponding to the Reidemeister *III*-moves in Virtual 1-knot theory. A virtual 2-knot diagram may be reduced to its bare combinatorial structure, forgetting all but the information that is invariant under isotopies of \mathbb{R}^3 and

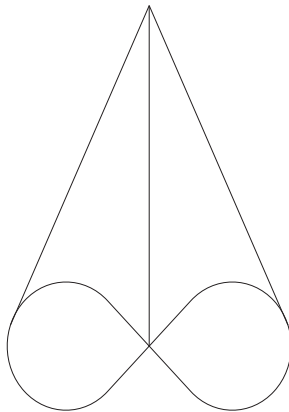


FIGURE 6.4. **Whitney-umbrella branch point**

F . In this regard, we do not distinguish diagrams that are related by isotopies of \mathbb{R}^3 and F .

Definition 6.3. ([41, section 3.5].) A virtual 2-knot diagram may be transformed by Roseman moves. There are seven types of local moves, shown here without crossing data. When a virtual 2-knot diagram undergoes a Roseman move, its crossing data carried continuously by the move. Two diagrams related by a series of Roseman moves are called *virtually equivalent*. The equivalence classes are *Virtual 2-knot types*, or sometimes simply *Virtual 2-knots*.

Note. The readers need not be familiar with Roseman moves in order to read this paper.

It is natural to ask whether we can define one-dimensional-higher tubes from virtual 2-knots since we succeed in the virtual 1-knot case as written in §§3-4.

The following facts let it be more natural: The one-dimensional-higher tube $\mathcal{E}(K)$ made from a virtual 1-knot K is the spun-knot of K if K is a classical knot (see [40]).

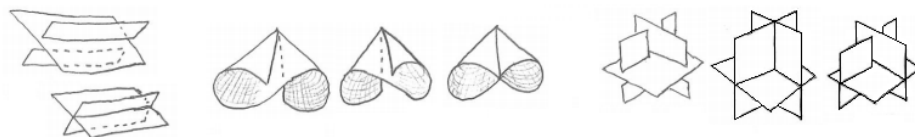


FIGURE 6.5. The singular point sets of virtual 2-knots

[45] defined spun-knots not only for classical 1-knot but also for classical 2-knots.

Question 6.4. Can we define one-dimensional-higher tubes for virtual 2-knots in a consistent way? Suppose that these tubes are diffeomorphic to $F \times S^1$ if the virtual 2-knot is defined by F .

Note that Satoh's method in [40] did not say anything about the virtual 2-knot case. In the virtual 1-knot case, in [38], Rourke interpreted Satoh's method as we reviewed in Theorem 4.3 and Definition 4.4.

Note 6.5. In the virtual 2-dimensional knot case we also use the terms 'fiber-circle' and 'Rourke-fibration' in Definition 4.4.

Definition 6.6. Let M be a 3-dimensional compact submanifold of \mathbb{R}^5 . Regard \mathbb{R}^5 as $\mathbb{R}^3 \times \mathbb{R}^2$. We say that the submanifold M admits *Rourke fibration*, or that M is embedded *fibrewise* if $M \cap (p \times \mathbb{R}^2)$ is a collection of circles for any point $p \in \mathbb{R}^3$. We call the circles in $M \cap (p \times \mathbb{R}^2)$, *fiber circles*.

If we try to generalize Rourke's way to the virtual 2-knot case, we will do the following: Let α be a virtual 2-knot diagram. Let $\mu = 0, 1, 2, 3$. We give μ -copies of circle to any μ -tuple point in α , and construct the tube. Of course we determine the position of fiber-circles in each fiber plane by the property of the μ -tuple point (See [41, section 3.7.1] for detail). See Figure 6.6.

However we encounter the following situation. Let α be any virtual 1-knot diagram.

- (1) The case where α has no virtual branch point.
- (2) The case where α has a virtual branch point.

In the (1) case, we can make a tube by Rourke's way. See [41, section 3.7.1].

In the (2) case, however, [41] found it difficult to define a tube near any virtual branch point. Thus it is natural to ask the following two questions.

Question 6.7. Can we put fiber-circles over each point of any virtual 2-knot in a consistent way as written above, and make one-dimensional-higher tube?

Question 6.8. Is there a one-dimensional-higher tube construction which is defined for all virtual 2-knots, and which agrees with the way in the (1) case written above when there are no virtual branch points?

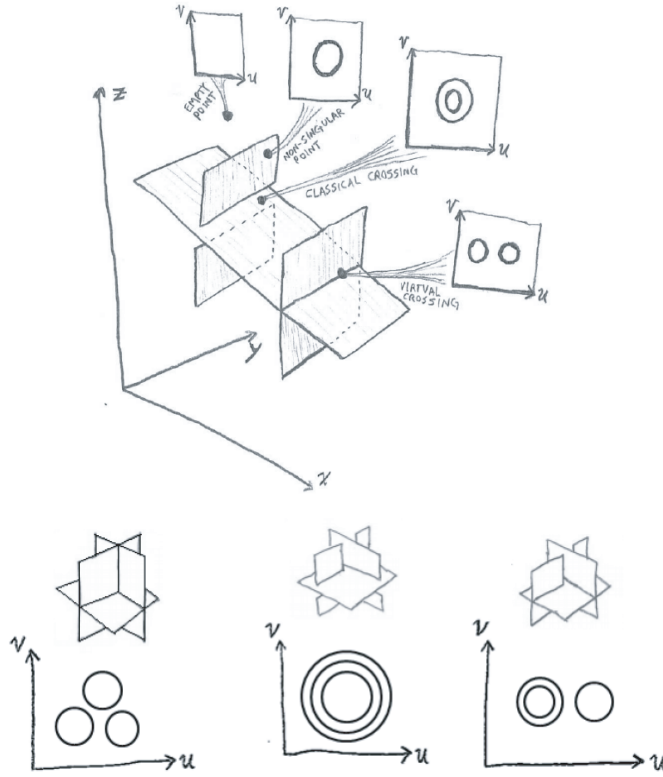


FIGURE 6.6. The nest of circles in fibers.

We generalize our method in §§3-4 and give an affirmative answer to Question 6.8, and hence to Question 6.4. See Theorem 6.16. We also use a spinning construction of submanifolds explained in Definition 3.1. Theorem 6.23 gives a negative answer to Question 6.7.

We make the virtual 2-knot version of representing surfaces, which are defined above Theorem 2.1.

Definition 6.9. ([41, section 3.5].) The development of an invariant for virtual 2-knot theory closely parallels that for virtual 1-knot theory. The idea is to think of a virtual

2-knot diagram as a classical 2-knot diagram “drawn” on a closed 3-manifold. We then define an equivalence relation on these objects that extends classical move-equivalence and allows the 3-manifold to vary. Take as input a virtual 2-knot diagram α . Let $N(\alpha)$ be a neighborhood of the diagram, which is a regular neighborhood except at virtual branch points, in the following sense: $N(\alpha)$ is formed by thickening α everywhere except at virtual branch points; as you approach virtual branch points, let the thickening gradually diminish to zero, so that near the virtual branch point $N(\alpha)$ looks like the cone over a thickened figure- ∞ .

Along each virtual crossing curve of α , double the square-shaped junction of $N(\alpha)$ to create overlapping “slabs”. Call this 3-manifold-with-boundary $B(\alpha)$. It has a purely classical knot diagram in it. (To be precise, $B(\alpha)$ is not technically a 3-manifold-with-boundary at virtual branch points, since the “slab” is pinched to zero thickness at these points.) See Figures 6.7 and 6.8.

Now embed $B(\alpha)$ into any compact oriented 3-manifold (not necessarily connected). The resultant compact 3-manifold is called a *representing 3-manifold* M associated with a virtual 2-knot diagram α . M contains a classical 2-knot diagram $\mathcal{I}(\alpha)$.

Note. Virtual 1-knot has two kinds of equivalent definitions: one is defined by using diagrams with virtual points in \mathbb{R}^2 . The other is done by using representing surfaces. See Theorem 2.1 and §2 of this paper, and [15, 16, 17]. It is very natural to ask the following question.

Question 6.10. Do we have the virtual 2-knot version of Theorem 2.1 by using representing 3-manifolds in Definition 6.9?

This question is open. [41] gave a partial answer. We do not discuss it in this paper.

Note that $\mathcal{I}(\alpha)$ is an immersed surface in an ordinary sense. That is, it does not include a virtual point. Note that we cannot embed a representing 3-manifold in \mathbb{R}^4 in general. We show an example. Take the Boy surface in \mathbb{R}^3 (see [3, 34]). We can regard it as a virtual 2-knot diagram as follows: Suppose that the only one immersed crossing curve is a virtual one. That is, it consists of one virtual triple point and other virtual double points. Then no representing 3-manifolds for this virtual 2-knot can be embedded in \mathbb{R}^4 . It is proved by using obstruction classes of the normal bundle of $\mathbb{R}P^2$ in \mathbb{R}^4 .

However, by [9], we have the following.

Theorem 6.11. *Any M in Definition 6.9 can be embedded in \mathbb{R}^5 .*

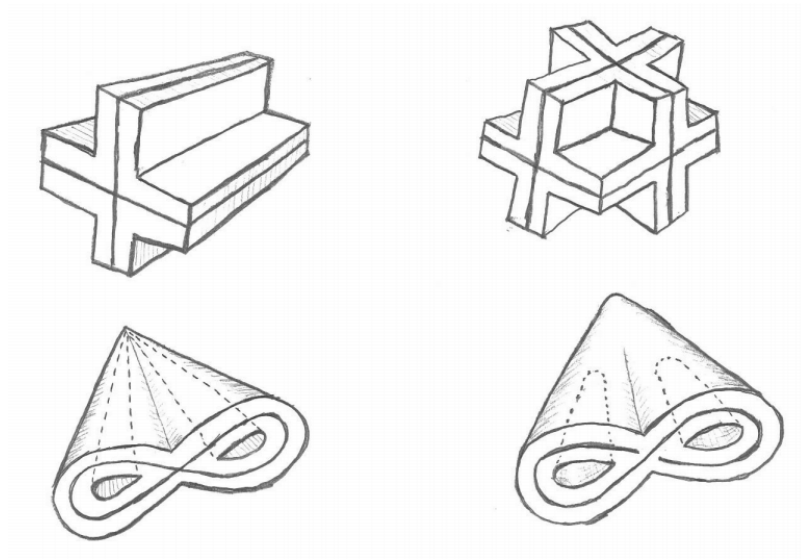


FIGURE 6.7. The left upper figure is a part of $N(\alpha)$ near a double point curve. The right upper figure is that near a triple point. The left lower figure is that near a virtual branch point. The right lower figure is that near a classical branch point.

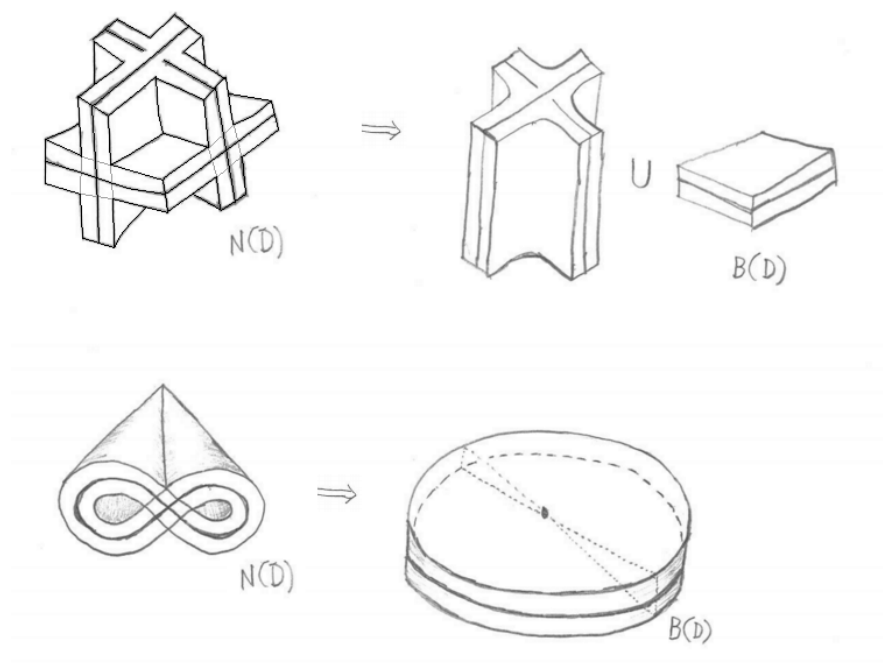


FIGURE 6.8. Make $B(\alpha)$ from $N(\alpha)$.

We will define the virtual 2-knot version of $\mathcal{E}(\alpha)$ in Definition 6.15 after some preliminaries. Let X be a 3-dimensional closed oriented abstract manifold. Let G_1 and G_2 be submanifolds of S^5 which are diffeomorphic to X . Recall the following fact

Claim 6.12. *There is a case that the submanifolds, G_1 and G_2 , of S^5 are non-isotopic.*

Proof of Claim 6.12. Take a spherical 3-knot K whose Alexander polynomial is non-trivial. Let G_2 be the knot-sum of G_1 and K . See e.g [37] for the Alexander polynomial of 3-knots and the knot-sum. \square

While G_1 and G_2 may be non-isotopic submanifolds, which are diffeomorphic to X above, of S^5 , it is the case that they are isotopic after removing an open three-ball from each of them. Let X_i° denote $X - (\text{an open 3-ball})$. Let $G_i^\circ = G_i - (\text{an open 3-ball})$ be a submanifold of S^5 ($i = 1, 2$).

Claim 6.13. *The submanifolds, G_1° and G_2° , of S^5 are isotopic.*

Note. Claim 6.13 is the virtual 2-knot version of Claim 4.6.

Proof of Claim 6.13. X° has a handle decomposition which consists of one 0-handle, 1-handles, 2-handles and no 3-handle. The dimensions of the cores of these handles are 0, 1, or 2. Hence the dimensions ≤ 2 . (Here, it is important the dimension $\neq 3$.) The dimension of S^5 is 5. Since $2 < \frac{3(2+1)}{2}$, Claim 6.13 holds by [8]. \square

Claim 6.14. *Let M be a compact 3-manifold. By Theorem 6.11, M is embedded in \mathbb{R}^5 . The normal bundle ν of M embedded in \mathbb{R}^5 is the trivial bundle for any embedding of M in \mathbb{R}^5 .*

Proof of Claim 6.14. If M is closed, M bounds a Seifert hypersurface V in S^5 (See [23, Theorem 2 page 49]). Take the normal bundle α of V in \mathbb{R}^5 . Then ν is a sum of vector bundles $\alpha|_M$ and an orientable \mathbb{R} -bundle over M . Hence Claim 6.14 holds in this case.

In the case where M is nonclosed, take the double DM of M as abstract manifolds. Then DM can be embedded in \mathbb{R}^5 . By the previous paragraph, the normal bundle of this embedded DM is trivial. Then the restriction of this normal bundle to $M \subset DM$ is trivial. By this fact and Claim 6.13, Claim 6.14 holds in this case. This completes the proof of Claim 6.14. \square

We introduce the virtual 2-knot version of $\mathcal{E}(\alpha)$.

Definition 6.15. Take an abstract manifold M in Definition 6.9, where $\mathcal{I}(\alpha)$ is still contained in M . Make $M \times [0, 1]$. We can obtain an embedded surface $\mathcal{J}(\alpha)$ contained in $M \times [0, 1]$ such that the projection of $\mathcal{J}(\alpha)$ by the projection $M \times [0, 1] \rightarrow M$ is

$\mathcal{I}(\alpha)$. We suppose $\mathcal{J}(\alpha) \cap (M \times \{0\}) = \emptyset$. Take any embedding of M in \mathbb{R}^5 . Define a submanifold $\mathcal{E}(\alpha)$ contained in S^5 to be the spinning submanifold made from $\mathcal{J}(\alpha)$ around M . (Recall Claim 6.14.)

We prove the virtual 2-knot version of Theorem 3.3, which is Theorem 6.16.

Theorem 6.16 is one of our main results. It gives an affirmative answer to Question 6.4.

Theorem 6.16. *Let α and α' be virtual 2-knot diagrams which represent the same virtual 2-knot. Make $\mathcal{E}(\alpha)$ and $\mathcal{E}(\alpha')$ by using a representing 3-manifold M (respectively, M') associated with α (respectively, α'). Then submanifolds, $\mathcal{E}(\alpha)$ and $\mathcal{E}(\alpha')$, of \mathbb{R}^5 are isotopic even if M is not diffeomorphic to M' .*

Proof of Theorem 6.16. It suffices to prove the following two cases:

- (i) α is obtained from α' by one of classical moves.
- (ii) α is obtained from α' by one of virtual moves.

In the case (ii), there is a diffeomorphism map $f : M \rightarrow M'$ such that $f(\alpha)$ is isotopic to α' in M' . Note that $\alpha \subset M$ and that $\alpha' \subset M'$.

In the case (i). Take a closed 3-ball B where the classical move is carried out. Note that $M \cup B$ (respectively, $M' \cup B$) is a representing 3-manifold of α (respectively α'). Note that there is a diffeomorphism map $f : M \cup B \rightarrow M' \cup B$ such that $f(\alpha)$ is isotopic to α' in $M' \cup B$. Note that $\alpha \subset M \cup B$ and that $\alpha' \subset M' \cup B$.

In both cases, by the following Theorem 6.18, Theorem 6.16 holds. \square

We prove the following Theorem 6.17, which is the virtual 2-knot version of Theorem 4.7. The key idea of the proof is Claim 6.13 (recall Note below Claim 6.13.) Let $i = 1, 2$. Take G_i defined in Claim 6.13. We can regard the tubular neighborhood of G_i in S^5 as $G_i \times D^2$. Embed a closed oriented surface in $G_i \times [0, 1]$, where we regard $[0, 1]$ as a radius of D^2 , and call the image J_i . Assume that $J_i \cap (G_i \times \{0\}) = \emptyset$. Suppose that there is a bundle map $\tilde{\sigma} : G_1 \times D^2 \rightarrow G_2 \times D^2$ such that $\tilde{\sigma}$ covers an orientation preserving diffeomorphism map $\sigma : G_1 \rightarrow G_2$ and such that $\tilde{\sigma}(J_1) = J_2$. Define a submanifold E_i contained in S^5 to be the spinning submanifold made from J_i by the rotation in $G_i \times D^2$.

Theorem 6.17. *The submanifolds, E_1 and E_2 , of S^5 are isotopic.*

Proof of Theorem 6.17. We can suppose that $J_i \subset G_i^\circ \times [0, 1]$. By the existence of σ , there is a bundle map $\tilde{\tau} : G_1^\circ \times D^2 \rightarrow G_2^\circ \times D^2$ such that $\tilde{\tau}$ covers a diffeomorphism map $\tau : G_1^\circ \rightarrow G_2^\circ$ and such that $\tilde{\tau}(J_1) = J_2$.

Note the following: Let $f : M^\circ \rightarrow S^5$ be an embedding map. We can regard τ as a diffeomorphism map $M^\circ \rightarrow M^\circ$. By Claim 6.13, the submanifolds, $f(M^\circ)$ and $f(\tau(M^\circ))$, of S^5 are isotopic. Therefore the submanifolds, E_1 and E_2 , of S^5 are isotopic. \square

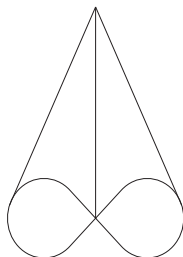


FIGURE 6.9. The intersection of a classical or virtual branch point and its neighborhood explained in Definition 6.19

Theorem 6.18. *Replace the condition that M is a closed compact oriented 3-manifold with the condition that M is a non-closed compact oriented 3-manifold. Then Theorem 6.17 also holds.*

Proof of Theorem 6.18. The proof of Theorem 6.18 is done in a similar fashion to that of Theorem 6.17. The proof of Theorem 6.18 is easier than that of Theorem 6.17. \square

We now have completed the proof of Theorem 6.16, and answered Question 6.4.

We next answer Question 6.8.

We define a consistent way to put a representing 3-manifold in \mathbb{R}^5 .

Definition 6.19. Let α be a virtual 2-knot diagram contained in \mathbb{R}^3 . Regard \mathbb{R}^3 as $\mathbb{R}^3 \times \{0\} \times \{0\} \subset \mathbb{R}^5 = \mathbb{R}^3 \times \mathbb{R} \times \mathbb{R}$. Put ‘a representing 3-manifold for α ’ in \mathbb{R}^5 as follows.

Take the neighborhood T of α as defined in Definition 6.9. Take a neighborhood of each of classical and virtual branch points such that the neighborhood is diffeomorphic to the closed 3-ball and such that $\alpha \cap (\text{the neighborhood})$ is as drawn in Figure 6.9.

Let $T' = T - \text{Int}(\text{the neighborhoods of real branch points and those of virtual branch ones})$. Along any virtual crossing line we double T' as done in Definition 6.9. Note that this operation can be done in \mathbb{R}^5 although it cannot be done in \mathbb{R}^4 in general. Thus we obtain a compact oriented 3-dimensional submanifold $X \subset \mathbb{R}^5$ from T' .

For a real branch point, we attach ‘the closed 3-ball which is a neighborhood of the real branch point’ to X . Note that near any virtual branch point, the operation can be done in $\mathbb{R}^3 \times \mathbb{R} \times \{0\}$. For a virtual branch point, we attach ‘the closed 3-ball which is

a neighborhood of the virtual branch point', as drawn in Figures 6.10-6.13, to X . Note that in Figures 6.10-6.13 we draw $\mathbb{R}^4 = \mathbb{R}^3 \times \mathbb{R} \times \{0\}$. Note that the virtual branch point vanishes in this closed 3-ball.

The resultant compact oriented 3-manifold is a representing 3-manifold with $\mathcal{I}(\alpha)$, which is defined in Definition 6.9. We call it M_ι . Recall that $\mathcal{I}(\alpha)$ has no virtual point and, in particular, that $\mathcal{I}(\alpha)$ has no virtual branch point.

Figure 6.10 draws a part of a representing 3-manifold M near a virtual branch point.

Figure 6.11 adds a part of $\mathcal{I}(\alpha)$ to Figures 6.10.

Figure 6.12 draws Figures 6.10 by seeing from a different direction.

Figure 6.13 draws Figures 6.11 by seeing from a different direction.

We prove that we have an affirmative answer to Question 6.8.

Theorem 6.20. *Let α be a virtual 2-knot diagram. Make $\mathcal{E}(\alpha)$ by using M_ι , and call it $\mathcal{E}_\iota(\alpha)$. If α has no virtual branch point, then $\mathcal{E}_\iota(\alpha)$ admits Rourke fibration.*

Proof of Theorem 6.20. Let $p \in \alpha$. Regard \mathbb{R}^5 in Definition 6.19 as $\mathbb{R}^3 \times \mathbb{R} \times \mathbb{R}$. By the construction of $\mathcal{E}_\iota(\alpha)$, $\mathcal{E}_\iota(\alpha) \cap (p \times \mathbb{R} \times \mathbb{R})$ is the empty set or a collection of circles such that this correspondence satisfies Rourke's description. Hence Theorem 6.20 holds. \square

Note 6.21. It is trivial that if we use another embedding of another M , $\mathcal{E}(\alpha)$ associated with the embedding may not admit Rourke fibration. Such an example exists. Let ξ be the trivial 2-knot diagram. It is trivial that ξ admits Rourke fibration. Let ζ be a virtual 2-knot diagram of the trivial 2-knot. Assume that the singular point set of ζ consists of two virtual branch points and one virtual segment.

A *virtual segment* is the segment with the following properties. It is a segment included in a virtual 2-knot diagram. One of the boundary is a virtual branch point. The points in the interior of the segment are virtual double points. It is drawn in Figure 6.15. It is drawn in Figure 6.4 if the branch point there is a virtual branch point. See [41].

ζ does not admit Rourke fibration by Theorem 6.23.

Note the following claim.

Claim 6.22. *Take $\mathcal{E}_\iota(\alpha)$ in Theorem 6.20. If α includes a virtual branch point, $\mathcal{E}_\iota(\alpha)$ does not admit Rourke's fibration. That is, $\mathcal{E}_\iota(\alpha)$ is not embedded fiberwise.*

Note. It is trivial that if we use another embedding of another M , $\mathcal{E}(\alpha)$ associated with the embedding may admit Rourke fibration. Such an example exists. It is the one in Note 6.21.

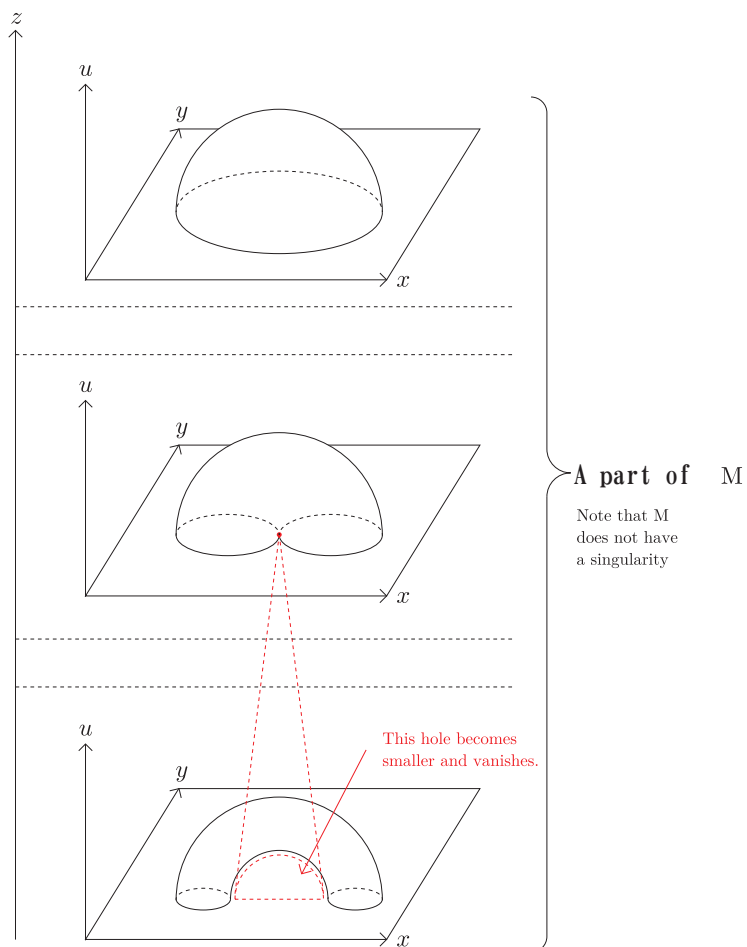


FIGURE 6.10. **A part of a representing 3-manifold near a virtual branch point. We do not draw a virtual branch point here. In 6.11 we do it.**

Proof of Claim 6.22. By Theorem 6.23. □

We give an alternative proof of Claim 6.22 after Proof of Theorem 6.23.

Theorem 6.23 is an answer to Question 6.7, and is one of our main results.

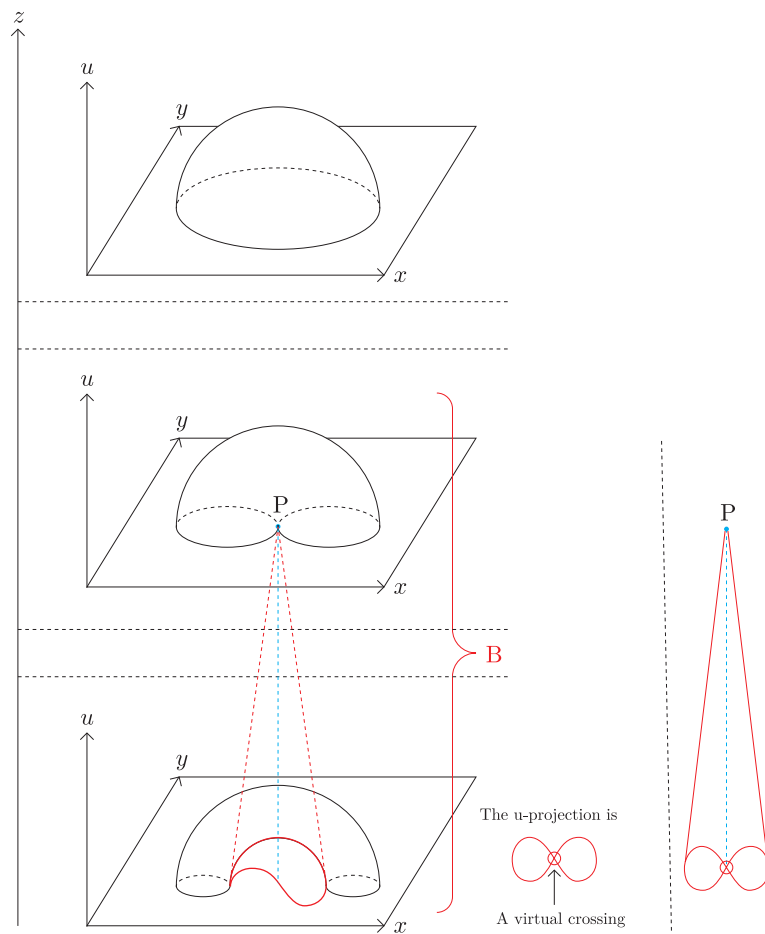


FIGURE 6.11. A part of a representing 3-manifold near a virtual branch point. We draw a virtual branch point here.

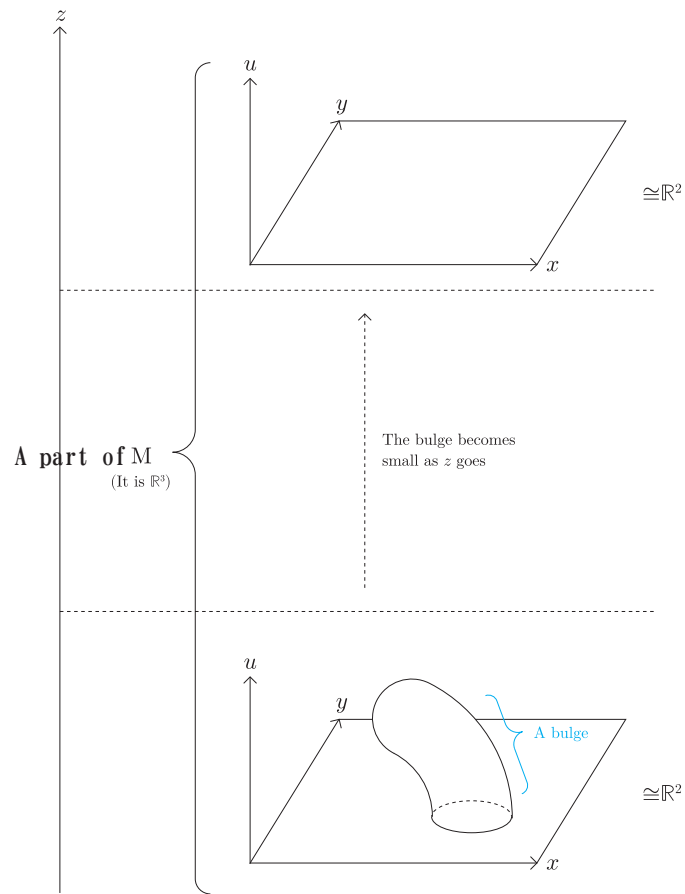


FIGURE 6.12. A part of a representing 3-manifold near a virtual branch point. We do not draw a virtual branch point here. In Figure 6.13 we will do it.

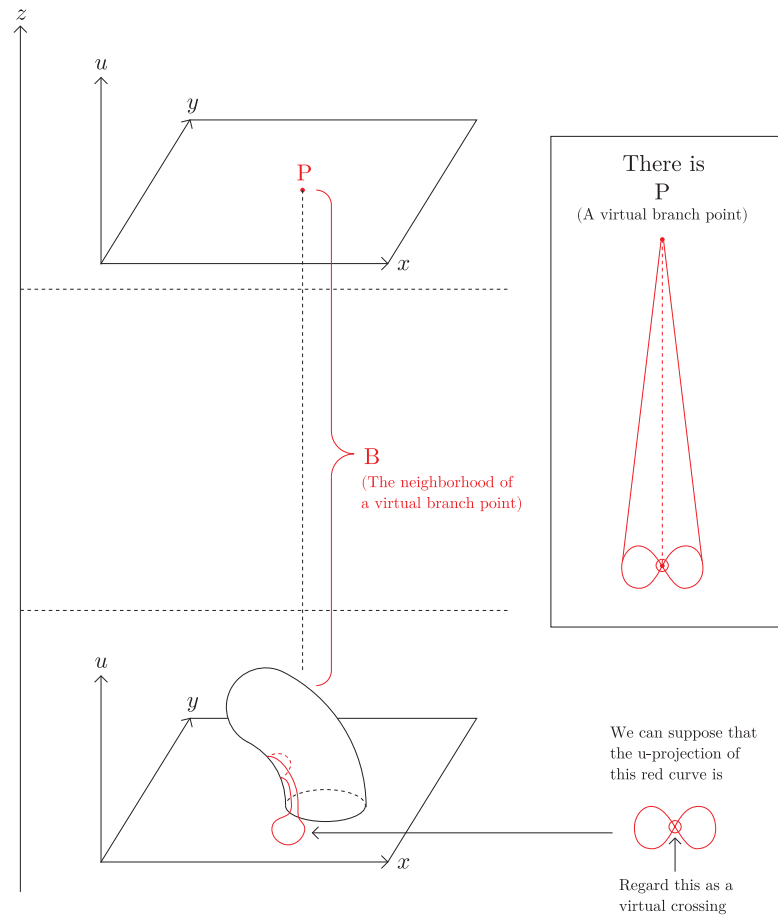


FIGURE 6.13. A part of a representing 3-manifold near a virtual branch point. We draw a virtual branch point here. We explain the most lower figure in more detail in Figure 6.14.

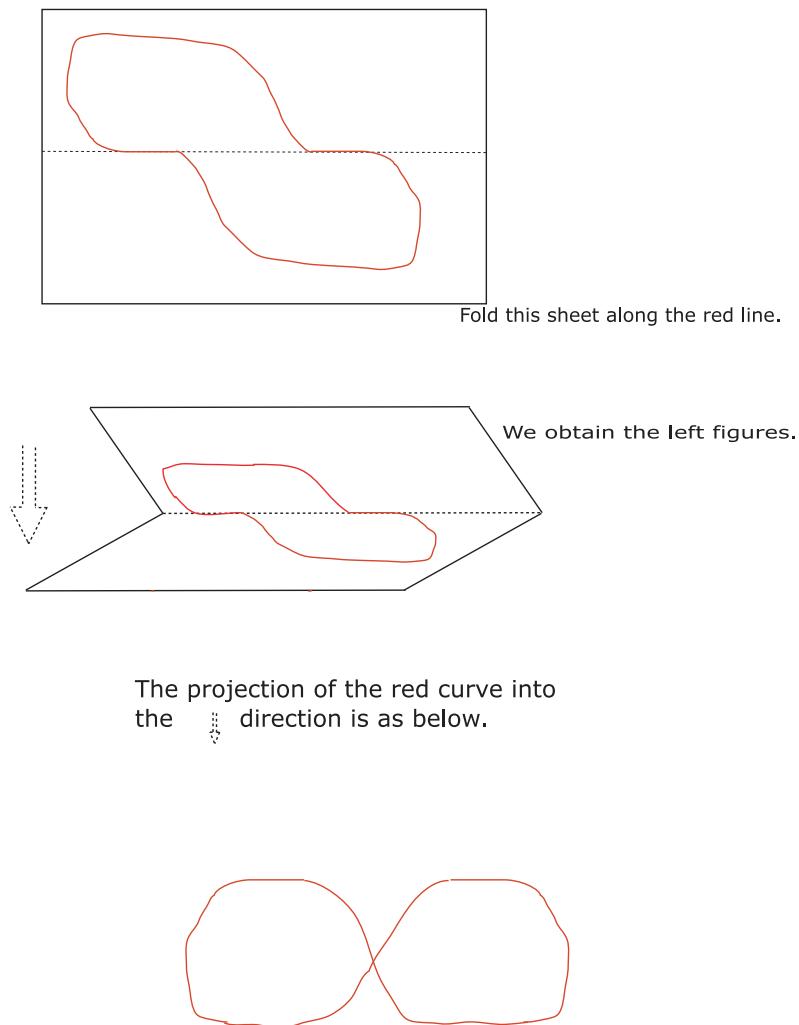


FIGURE 6.14. The explanation of the most lower figure of Figure 6.13. The neighborhood of the red curve of that figure is obtained by curving the middle figure of the above figures.

Theorem 6.23. *The answer to Question 6.7 is negative.*

Proof of Theorem 6.23. We prove by ‘reductio ad absurdum’. We suppose the following assumption, and will arrive at a contradiction.

Assumption. The neighborhood of a virtual branch point can be covered by the fiber-circles.

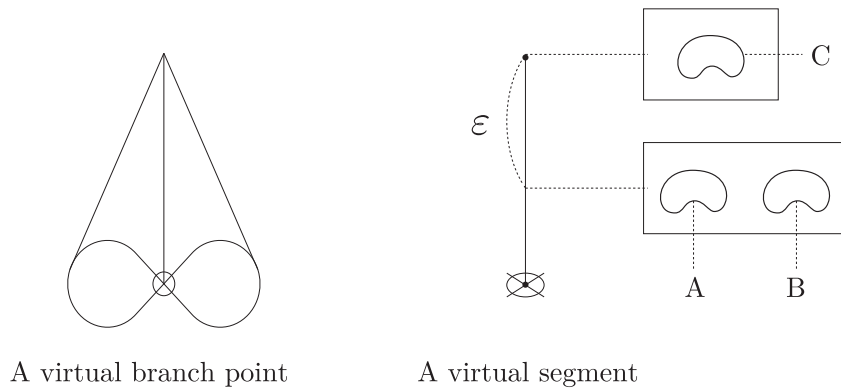


FIGURE 6.15. **The assumption of ‘reductio ad absurdum’**

Note the fiber over the virtual segment as shown in Figure 6.15.

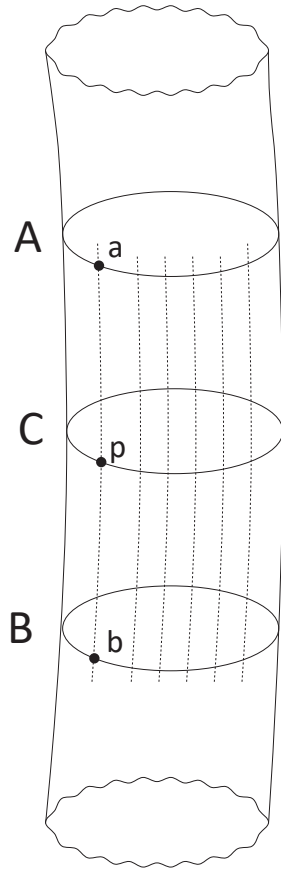
Give a Euclidean metric to \mathbb{R}^5 .

By Assumption, the circles, A and B in Figure 6.15, meet at the circle C when $\varepsilon \rightarrow 0$. Let s be the area of C . When $\varepsilon \rightarrow 0$, $A \rightarrow C$ and $B \rightarrow C$. Hence, we have the following.

$$(6.1) \quad \text{When } \varepsilon \rightarrow 0, (\text{the area of } B) \rightarrow s.$$

Note that s is a fixed positive real number.

Take a one-parameter-family for each point $p \in C$. See Figure 6.16. Suppose that a and b go to p when $\varepsilon \rightarrow 0$. Let $\delta(a, b)$ the distance along the trace of the one-parameter-family



By the assumption of
 'reductio ad absurdum',
 there is a cylinder like this.

FIGURE 6.16. **A one parameter families**

between a and b .

$$(6.2) \quad \text{When } \varepsilon \rightarrow 0, \delta(a, b) \rightarrow 0.$$

In the fiber \mathbb{R}^2 which includes A and B , take any point $x \in A$. Suppose that x goes to $y \in B$ by the one-parameter-family. In this fiber \mathbb{R}^2 take a disc of radius $2\delta(x, y)$ whose center is $x \in A$. Call the sum of the discs, $N(A)$. See Figure 6.17. When $\varepsilon \rightarrow 0$, (the area of $N(A)$) $\rightarrow 0$. By (6.2), $B \subset N(A)$. Note that in this fiber \mathbb{R}^2 , B (respectively,

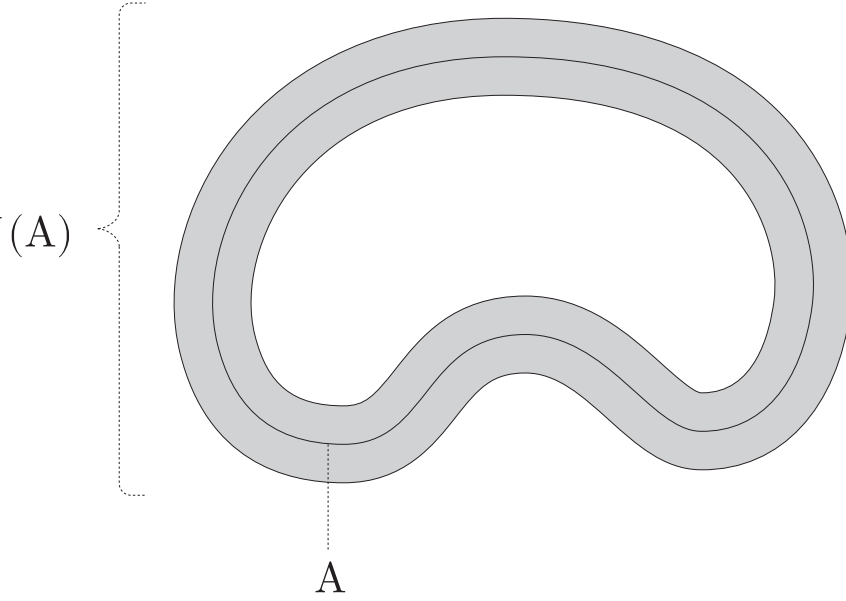


FIGURE 6.17. $N(A)$

A) is not included in the inside of A (respectively, B). Therefore, by Jordan curve theorem, the inside of B is also included in $N(A)$. Hence we have the following.

(6.3) When $\varepsilon \rightarrow 0$, (the area of B) $\rightarrow 0$.

By (6.1) and (6.3), we arrived at a contradiction.

This completes the proof of Theorem 6.23. \square

We give a direct proof of why $\mathcal{E}_t(\alpha)$ does not admit Rourke fibration, without using Theorem 6.23. Note that it is not an alternative one of Theorem 6.23.

Alternative proof of Claim 6.22. If p is a virtual branch point, p is in the boundary of a virtual segment in \mathbb{R}^3 . Take $\mathcal{I}(\alpha)$ immersed in M . Let $\kappa : \mathcal{I}(\alpha) \rightarrow \alpha$ be the natural map defined in Definition 6.3. We have the following. $\kappa^{-1}(\text{the virtual segment})$ is a union

of two segments, Ψ and Φ . A point of $\partial\Psi$ and that of $\partial\Phi$ meet at a point as drawn in Figure 6.18. κ (this point) is the virtual branch point.

The two segments make an angle. See Figures 6.10-6.13. The angle is acute. Even if we take an arbitrary representing 3-manifold of the virtual 2-knot diagram α , the angle is acute not obtuse. Furthermore the angle is put as drawn there. The reason for this is that there is always an acute angle as drawn in Figure 6.18 whichever representing 3-manifolds we take.

As we preannounced in Notes 4.2 and 4.5, we use Figures 4.2 and 4.3. In particular, see the most lower figure of Figure 4.3.

Therefore $\mathcal{E}_i(\alpha) \cap (p \times \mathbb{R}_u \times \mathbb{R}_v)$ is a bouquet, not the empty set or a collection of circles.

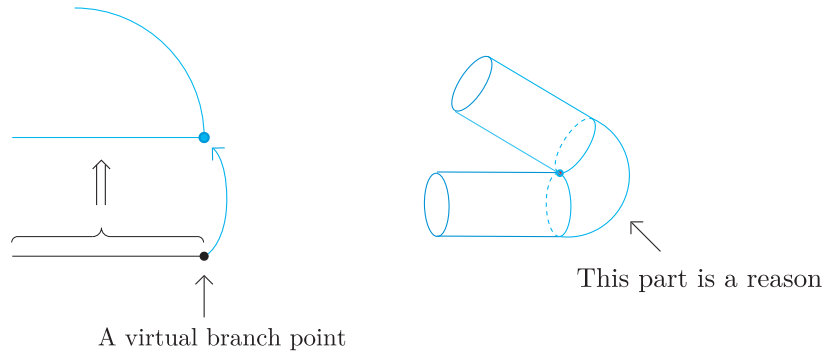


FIGURE 6.18. $\mathcal{E}_\iota(\alpha)$ made by the spinning construction can be embedded in \mathbb{R}^5 but $\mathcal{E}_\iota(\alpha)$ does not admit Rourke fibration. The reason why we cannot make the fiber over any virtual branch point a collection of circles is drawn.

Therefore Claim 6.22 holds. □

7. THE \mathcal{E} -EQUIVALENCE

We introduce a new equivalence relation of the set of 1-(respectively, 2-)dimensional virtual knots.

Definition 7.1. Let K and J be 1-(respectively, 2-)dimensional virtual knots. If the submanifolds, $\mathcal{E}(K)$ and $\mathcal{E}(J)$, of \mathbb{R}^4 (respectively, \mathbb{R}^5) are isotopic, K and J are said to be \mathcal{E} -equivalent. See Theorem 6.16, and the line right below Theorem 3.3 for $\mathcal{E}(\quad)$.

Theorem 7.2. (By [38, Theorem 2.2] and [40, Proposition 3.3].) *If two virtual 1-knots are welded equivalent, then they are \mathcal{E} -equivalent. Hence there are two virtual 1-knots, J and K , such that J is not virtually equivalent to K but such that $\mathcal{E}(J)$ is isotopic to $\mathcal{E}(K)$.*

Proof of Theorem 7.2. By [38, Theorem 2.2], there are two virtual 1-knots, J and K , such that J is not virtually equivalent to K but such that J is welded equivalent to K . By [40, Proposition 3.3], J and K are \mathcal{E} -equivalent. \square

Thus it is natural to ask whether we have the virtual 2-knot version of Theorem 7.2. In other words, are there virtual 2-knots, J and K , which are \mathcal{E} -equivalent but which are not virtually equivalent? We answer this question below.

Let α be a 1-dimensional virtual knot diagram defined in \mathbb{R}^2 . Regard \mathbb{R}^3 as the result of rotating $\mathbb{R}_{\geq 0}^2 = \mathbb{R}^1 \times \{t|t \geq 0\}$ around $\mathbb{R}^1 \times \{t|t = 0\}$ as the axis. Take α in $\mathbb{R}^1 \times \{t|t > 0\}$. When we rotate $\mathbb{R}_{\geq 0}^2$, rotate α together. Then we obtain a 2-dimensional virtual knot diagram in \mathbb{R}^3 naturally, and call it $\mathcal{O}(\alpha)$. Note that $\mathcal{O}(\alpha)$ is a virtual 2-knot diagram made from T^2 .

If 1-dimensional virtual knot diagrams, α and β , are virtually equivalent, it is trivial that 2-dimensional virtual knot diagrams, $\mathcal{O}(\alpha)$ and $\mathcal{O}(\beta)$ are virtually equivalent (see Definition 6.3). Hence it makes sense that we define an 2-dimensional virtual knot $\mathcal{O}(K)$ for a 1-dimensional virtual knot K .

Let X be a classical surface knot contained in $\mathbb{R}^4 = \mathbb{R}^3 \times \{t \in \mathbb{R}\}$. Take X in $\mathbb{R}^3 \times \{t > 0\}$. Regard \mathbb{R}^5 as the result of rotating $\mathbb{R}^3 \times \{t \geq 0\}$ around $\mathbb{R}^3 \times \{t = 0\}$ as the axis. Then we rotate X together. Call the resultant 3-dimensional submanifold of \mathbb{R}^5 , $\mathcal{O}(X)$. Note the following: If X is diffeomorphic to a closed surface Σ_g , then $\mathcal{O}(X)$ is diffeomorphic to $\Sigma_g \times S^1$.

Proposition 7.3. *Let K be a virtual 1-knot. Then the submanifolds, $\mathcal{E}(\mathcal{O}(K))$ and $\mathcal{O}(\mathcal{E}(K))$, of \mathbb{R}^5 are isotopic.*

Proof of Proposition 7.3. By the definitions. \square

The *standardly embedded torus* or *standard torus* is a submanifold of \mathbb{R}^4 , diffeomorphic to the torus, and put in the standard position. Let Σ_g be an oriented closed surface. The

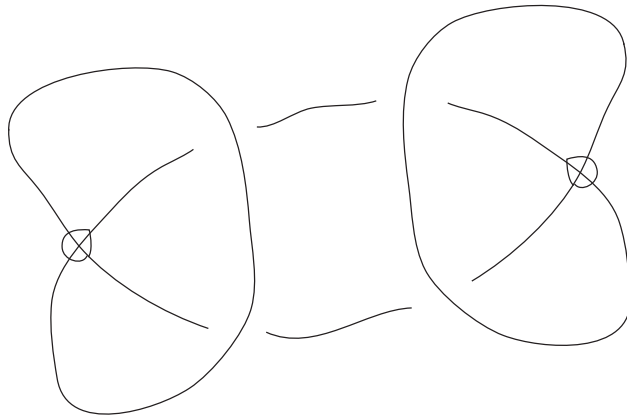


FIGURE 7.1. **Virtual reef knot**

standardly embedded surface (diffeomorphic to Σ_g) or standard surface (diffeomorphic to Σ_g) is defined as well. Note that we can regard classical 1- (respectively, 2-) knots as virtual knots.

Let R be the virtual reef knot whose diagram is drawn in [38, Figure 3, section three]. We cite the diagram in Figure 7.1. As written there, R is a nontrivial virtual 1-knot, is welded equivalent to the trivial 1-knot, and has the group \mathbb{Z} .

Claim 7.4. *The virtual 2-knot $\mathcal{O}(R)$ is not virtually equivalent to the standard torus.*

Note 7.5. The submanifold, $\mathcal{E}(R)$ and the standard torus, of \mathbb{R}^4 are isotopic because the virtual 1-knot R is welded equivalent to the unknot.

Proof of Claim 7.4. The proof is done in a similar way in [42] and a generalized fashion of the manner in [38, section three]: The fundamental group of the virtual reef knot R is \mathbb{Z} . However the fundamental group of the mirror image of R is non-trivial. The fundamental group of the mirror image of R is the lower fundamental group of $\mathcal{O}(R)$ and

its non-triviality demonstrates the non-triviality of $\mathcal{O}(R)$ as a virtual 2-knot. \square

Theorem 7.6 is one of our main results.

Theorem 7.6. *There is a virtual 2-knot K with the following conditions.*

- (1) *The virtual 2-knot K is not virtually equivalent to the standard surface.*
- (2) *The virtual 2-knot K is \mathcal{E} -equivalent to the standard surface.*

Proof of Theorem 7.6. Let K be the virtual 2-knot $\mathcal{O}(R)$ in Claim 7.4. Claim 7.4 implies Theorem 7.6.(1). Let T denote the standard torus. By Note 7.5, $\mathcal{E}(R) = T$. Proposition 7.3 implies $\mathcal{E}(K) = \mathcal{E}(\mathcal{O}(R)) = \mathcal{O}(\mathcal{E}(R)) = \mathcal{O}(T)$, where $=$ denotes the ambient isotopy of submanifolds. $\mathcal{O}(T)$ and $\mathcal{E}(T)$ are standardly embedded T^3 in \mathbb{R}^5 by the definition of them. Hence we have Theorem 7.6.(2). Therefore Theorem 7.6 holds. \square

We ask questions.

Question 7.7. (1) Do we have the following? Let Σ_g be a closed oriented genus g surface. Let Q (respectively, Q') be a virtual surface-knot made from Σ_g . If Q and Q' have the group \mathbb{Z} , then the submanifolds, $\mathcal{E}(Q)$ and $\mathcal{E}(Q')$, of \mathbb{R}^5 are isotopic.

(2) Is a virtual 1- (respectively, 2-) knot K welded equivalent to the trivial 1-knot if K has the group \mathbb{Z} ?

8. THE FIBREWISE EQUIVALENCE

8.1. The fibrewise equivalence is equal to the rotational welded equivalence, and is different from the welded equivalence of virtual 1-knots.

We research relations among the fiberwise equivalence of virtual 1-knots, the welded equivalence of them, and the rotational welded equivalence of them. We mentioned it in the last few paragraphs of §1.3. See [38, 40] for the definition of the welded equivalence, and [16, 18, 41] for that of the rotational welded equivalence, as we also mentioned them in the last few paragraphs of §1.3.

We first introduce the definition of the fiberwise equivalence of virtual 1-knots. For our purpose (to prove Theorems 8.5 and 8.48), we will modify the definition a few times as below.

Definition 8.1. Let α and β be virtual 1-knot diagrams. We say that α and β are *fiberwise equivalent* if Rourke's description of $\mathcal{S}(\alpha)$ and that of $\mathcal{S}(\beta)$ are 'fiberwise isotopic'.

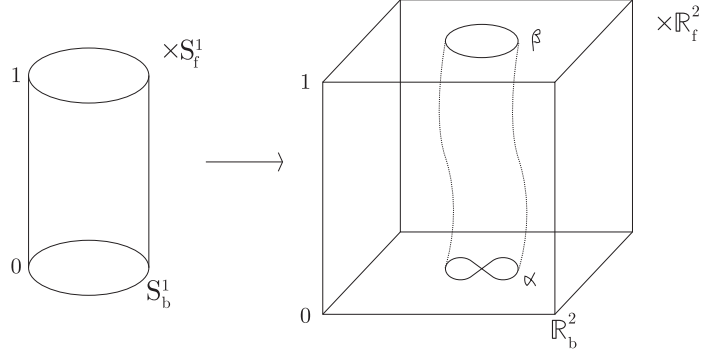


FIGURE 8.1. **Fiberwise isotopy**

In other words, this means that α and β satisfy the following conditions. There is an embedding map

$$g : S_b^1 \times [0, 1] \times S_f^1 \hookrightarrow \mathbb{R}_b^2 \times [0, 1] \times \mathbb{R}_f^2$$

with the following properties. See Figure 8.1.

- (1) For any fixed $t \in [0, 1]$, $g(S_b^1 \times \{t\} \times S_f^1) \subset \mathbb{R}_b^2 \times \{t\} \times \mathbb{R}_f^2$.
- (2) For any fixed $p \in S_b^1$ and any fixed $t \in [0, 1]$, $g(\{p\} \times \{t\} \times S_f^1)$ is contained in the same fiber $\{q\} \times \mathbb{R}_f^2$ for a point $q \in \mathbb{R}_b^2 \times [0, 1]$.
- (3) Let $\pi : \mathbb{R}_b^2 \times [0, 1] \times \mathbb{R}_f^2 \rightarrow \mathbb{R}_b^2 \times [0, 1]$. $(\pi \circ g)(S_b^1 \times \{0\} \times S_f^1)$ (respectively, $(\pi \circ g)(S_b^1 \times \{1\} \times S_f^1)$) $\subset \mathbb{R}_b^2 \times \{0\}$ (respectively, $\mathbb{R}_b^2 \times \{1\}$) is the diagram α (respectively, β) without information whether each crossing point is a classical one or a virtual one. This information is given by the fiber-circles over each crossing point as in Theorem 4.3 and Definition 4.4. $\pi \circ g$ meets $\mathbb{R}_b^2 \times \{0, 1\}$ transversely.

In knot theory we usually use an ‘ambient’ isotopy in order to define the equivalence relation of knots as below. We impose the following condition (4). (See [4, sections 1.1 and 1.2] for an explanation on this fact in the 1-dimensional classical knot case.)

(4) Let g_t denote

$$g|_{S_b^1 \times \{t\} \times S_f^1} : S_b^1 \times \{t\} \times S_f^1 \hookrightarrow \mathbb{R}_b^2 \times \{t\} \times \mathbb{R}_f^2$$

for $0 \leq t \leq 1$. There is an isotopy

$$H_t : \mathbb{R}_b^2 \times \{t\} \times \mathbb{R}_f^2 \rightarrow \mathbb{R}_b^2 \times \{t\} \times \mathbb{R}_f^2 (0 \leq t \leq 1)$$

such that H_0 is the identity map and such that $g_t = H_t \circ g_0$ for any $t \in [0, 1]$.

We call g a *special isotopy* between α and β .

Definition 8.2. Take g in Definition 8.1. If g' is obtained by moving g by an ambient isotopy map G_t , where $0 \leq t \leq 1$, $g_0 = g$, and $g_1 = g'$, keeping the conditions (1)-(4) of Definition 8.1, then we say that g' is *level preserving*, *fiberwise isotopic* or *special isotopic* to g , or that we *perturb g in the special way* to obtain g' . We write $g \sim g'$. G_t is called a *level preserving*, *fiberwise isotopy* or *special isotopy* between g and g' .

Note 8.3. The following holds. Let $\rho : S_b^1 \times [0, 1] \times S_f^1 \rightarrow S_b^1 \times [0, 1]$ be the natural projection. Then there is a (not necessarily smooth) continuous map $\underline{g} : S_b^1 \times [0, 1] \rightarrow \mathbb{R}^2 \times [0, 1]$ such that $\pi \circ g = \underline{g} \circ \rho$. That is, there is the following commutative diagram.

$$\begin{array}{ccc} S_b^1 \times [0, 1] \times S_f^1 & \xrightarrow{g} & \mathbb{R}_b^2 \times [0, 1] \times \mathbb{R}_f^2 \\ \downarrow \rho & \circlearrowleft & \downarrow \pi \\ S_b^1 \times [0, 1] & \xrightarrow{\underline{g}} & \mathbb{R}_b^2 \times [0, 1] \end{array}$$

Definition 8.4. Under the above condition, we say that \underline{g} is *covered* by g .

The following theorem is one of our main results.

Theorem 8.5. *Two virtual 1-knot diagrams α and β are smooth fiberwise equivalent if and only if α and β are smooth rotational welded equivalent.*

Note. See Note 8.44.

Proof of Theorem 8.5. The ‘if’ part is easy.

We prove the ‘only if’ part.

Strategy. See (I) and (II) below. We want to prove (I) \Leftrightarrow (II). It is easy to prove (II) \Rightarrow (I). We will prove (I) \Rightarrow (II) as follows.

(I) Smooth virtual 1-knot diagrams α and β are smooth fiberwise equivalent.

(II) Smooth virtual 1-knot diagrams α and β are smooth rotational welded equivalent.

See (1) below. In Claim 8.7 we will prove (I) \Rightarrow (1).

(1) There is a PL virtual 1-knot diagram α' (respectively, β') which is piecewise smooth isotopic to α (respectively, β) such that α' and β' are PL fiberwise equivalent.

See (2) below. In Theorem 8.39, we will prove (1) \Rightarrow (2). It will be proved in the text which starts from Proposition 8.10, and ends in Claim 8.40.

(2) α' and β' are PL rotational welded equivalent.

In Lemma 8.41, we will prove (2) \Rightarrow (II). Thus we will finish the proof of (I) \Rightarrow (II).

Assume that smooth virtual 1-knot diagrams α and β are smooth fiberwise equivalent. We do not know whether or not there are two special isotopies g and g' between α and β with the following properties. g and g' are not smooth special isotopic but piecewise smooth special isotopic. Although we do not answer this question, we accomplish the proof of (I) \Leftrightarrow (II).

Take g in Definition 8.1. We do not know whether there is a smooth g' with $g' \sim g$ with the following properties: There is a finite simplicial structure on $\text{Im } \pi \circ g'$ which restricts to a finite simplicial structure on the singular subset of $\text{Im } \pi \circ g'$. One reason is as follows. $\text{Im } \pi \circ g$ may be the projection of a wild embedding for a smooth g even if g is not a wild embedding map. Although we do not answer this question, we accomplish the proof of (I) \Leftrightarrow (II).

Definition 8.6. Consider the conditions of Definition 8.1 in the PL category. The equivalence relation is called *PL fiberwise equivalence*.

Claim 8.7. *If virtual 1-knot diagrams α and β are smooth fiberwise equivalence, then α and β are PL fiberwise equivalence.*

Proof of Claim 8.7. It is enough to prove that the map g in Definition 8.1 is approximated by a fiberwise level-preserving PL embedding map. We prove it below.

Regard S_b^1 as $[0, 1]/\sim$, where $0 \sim 1$. Regard S_f^1 as $[0, 1]/\sim$, where $0 \sim 1$. Hence we can regard $S_b^1 \times [0, 1] \times S_f^1$ as the one made from $[0, 1] \times [0, 1] \times [0, 1]$ by these equivalence relations.

Let n be any positive integer. Take points $(\frac{i}{2n}, \frac{j}{2n}, \frac{k}{2n}) \in [0, 1] \times [0, 1] \times [0, 1]$, where i (respectively, j, k) is any integer with the condition $0 \leq i$ (respectively, j, k) $\leq 2n$.

Let l be any integer with the condition $0 \leq 2l$ (respectively, $2l + 2 \leq 2n$). Take any cube C whose vertices are $(\frac{\alpha}{2n}, \frac{\beta}{2n}, \frac{\gamma}{2n})$, where α (respectively, β, γ) is any integer in $\{2l, 2l + 2\}$.

Take a simplicial division on $S_b^1 \times [0, 1] \times S_f^1$ as follows.

- (1) 0-simplices are all $(\frac{i}{2n}, \frac{j}{2n}, \frac{k}{2n}) \in [0, 1] \times [0, 1] \times [0, 1]$ as above.
- (2) 1-simplices are defined as follows. Take any cube C . Note that each of six sites includes nine 0-simplices, that the sum of six sites includes 26 0-simplices, and that C includes 27 0-simplices. Take the 0-simplex P in C which is not included in any site. Take any segment whose boundary is P and one of the other 28 0-simplices. Take 16 segments in each site of C as drawn in Figure 8.2. 1-simplices are these two kinds of segment.
- (3) The set of 1-simplices defines 2-simplices naturally.
- (4) The set of 2-simplices defines 3-simplices naturally.

Let n be sufficiently large. Take the image of all 0-simplices by g in $\mathbb{R}_b^2 \times [0, 1] \times \mathbb{R}_f^2$. They determine a fiberwise level-preserving PL embedding map of $S_b^1 \times [0, 1] \times S_f^1$ naturally. *Reason.* $\text{Im } g$ is a smooth regular submanifold. Hence it has a tubular neighborhood.

This completes the proof of Claim 8.7. \square

Note 8.8. If $C = (\text{Im } g) \cap (\text{a fiber } \mathbb{R}_f^2)$ is PL homeomorphic to a circle, then C is a polygon. However the number of the vertices of C depends on fibers.

Note 8.9. From here to the end of the proof of Theorem 8.39, we work in the PL category unless we indicate otherwise. After that, we will go back to the smooth category.

When we move a map by isotopy, we take a PL subdivision if necessary.

Claim 8.7 implies the following.

Proposition 8.10. *g in Definition 8.6 satisfies the condition that a finite simplicial structure on $\text{Im } \pi \circ g$ which restricts to a finite simplicial structure on the singular subset of $\text{Im } \pi \circ g$.*

We call the operation drawn in Figure 8.3, the Δ^1 -move of virtual 1-knot diagrams. Note that we do not draw the other part of this diagram. The other part may intersect the part drawn in Figure 8.3. By Proposition 8.10, α, β in Definition 8.6 have the following properties:

Claim 8.11. *α (respectively, β) is obtained from β (respectively, α) by a finite step of Δ^1 -moves.*

Definition 8.12. Add the following condition to Definition 8.6 without changing the other parts. (Note we work in the PL category.)

(8.12.1) In each fiber \mathbb{R}_f^2 , there are a finite number of circles. (That is, $< \infty$.)

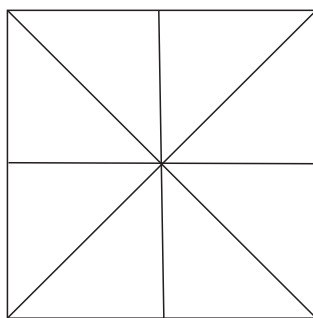


FIGURE 8.2. **16 1-simplices on a site of C**

Note. See Note 8.42. Recall Note 8.8.

Indeed, the following holds.

Theorem 8.13. *Definitions 8.6 and 8.12 are equivalent.*

Proof of Theorem 8.13. It is trivial that if g satisfies Definition 8.12, then g satisfies Definition 8.6. We prove that if g satisfies Definition 8.6, then we can perturb g in the special way so that g satisfies Definition 8.12. Suppose that g satisfies Definition 8.6.

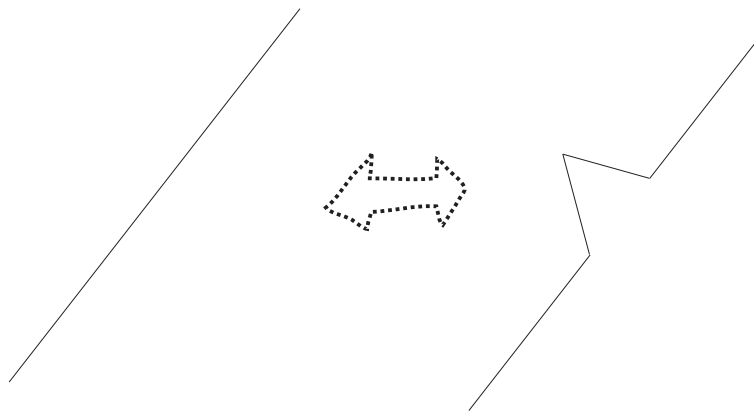


FIGURE 8.3. The Δ^1 -move.

Let $q \in \mathbb{R}_b^2$ and $t \in [0, 1]$. Since $\text{Im}g$ is a compact PL regular submanifold, $\text{Im}g \cap (\{q\} \times \{t\} \times \mathbb{R}_f)$ is a disjoint union of a finite number of circles and a finite number of annuli. Note that the union of them is a regular submanifold of $\{q\} \times \{t\} \times \mathbb{R}_f^2$. Take a tubular neighborhood N of each annulus in $\mathbb{R}_b^2 \times [0, 1] \times \mathbb{R}_f^2$, to be small enough. Stretch each annulus into the direction perpendicular to $\{x\} \times \{t\} \times \mathbb{R}_f^2$. Then we can obtain a new g which satisfies Definition 8.12. The idea of how we stretch is drawn in Figure 8.4. Note that Figure 8.4 draws ‘figures in PL category’ although the figures are smoothened. \square

A point $p \in \text{Im}\pi \circ g = (\pi \circ g)(S_b^1 \times [0, 1] \times S_f^1) = (\underline{g} \circ \rho)(S_b^1 \times [0, 1] \times S_f^1) = \underline{g}(S_b^1 \times [0, 1])$ is called a *multiple point* or *n-tuple point* if $\underline{g}^{-1}(p) \in S_b^1 \times [0, 1]$ consists of n points ($n \geq 2$). (Note that in Definition 8.12, $n < \infty$.) A point $p \in \text{Im}\pi \circ g$ is called a *single point* if $\underline{g}^{-1}(p)$ consists of a single point. The *singular point set* of $p \in \text{Im}\pi \circ g$ consists of branch points and multiple points.

Note the following facts. Take g in Definition 8.12, and \underline{g} which is covered by g . Recall that ‘cover’ is defined in Definition 8.4. Suppose that \underline{g} is a generic map. Note $\text{Im} \underline{g}$. We can define whether each double point is classical or virtual by using the information of the fiber-circles over each point as in Theorem 4.3, Definition 4.4, Note 6.5, and Definition 6.6. There is a case where a classical (respectively, virtual) double point appears. The information of fiber-circles over each branch point determines that the branch point is classical. *Reason.* By Theorem 6.23, there are no virtual branch point.

Note each triple point. There are three circles in the fiber over each triple point. There are four cases how three circles are put in the fiber. See Notes 8.14 and 8.16, Definition 8.15, and Figure 8.5. There is a case where each of the four occurs.

Note 8.14. $(\pi \circ g)(S_b^1 \times [0, 1] \times S_f^1)$ in $\mathbb{R}_b^2 \times [0, 1]$ is a welded 2-knot with a fixed boundary in general, and is not a virtual 2-knot with a fixed boundary in general. See [41, sections 3.5-3.7] for their definitions and their difference. In the welded 2-knot case we also use the terms, ‘fiber-circle’ and ‘Rourke-fibration’. See Note 8.16.

Here we cite the definition of welded 2-knots from [41].

Recall that a 2-knot diagram is (the image of) a generic map of a surface in 3-space, with classical and virtual crossing data along the double-point arcs. Also recall that 2-knot diagrams may be transformed by Roseman moves, which preserve the crossing data locally.

Definition 8.15. ([41, section 3.6].) If all triple points of a 2-knot diagram are of the four types shown in Figure 8.5, the diagram is called a Welded 2-knot diagram. If a pair of Welded 2-knot diagrams are related by a series of Roseman moves, with only Welded

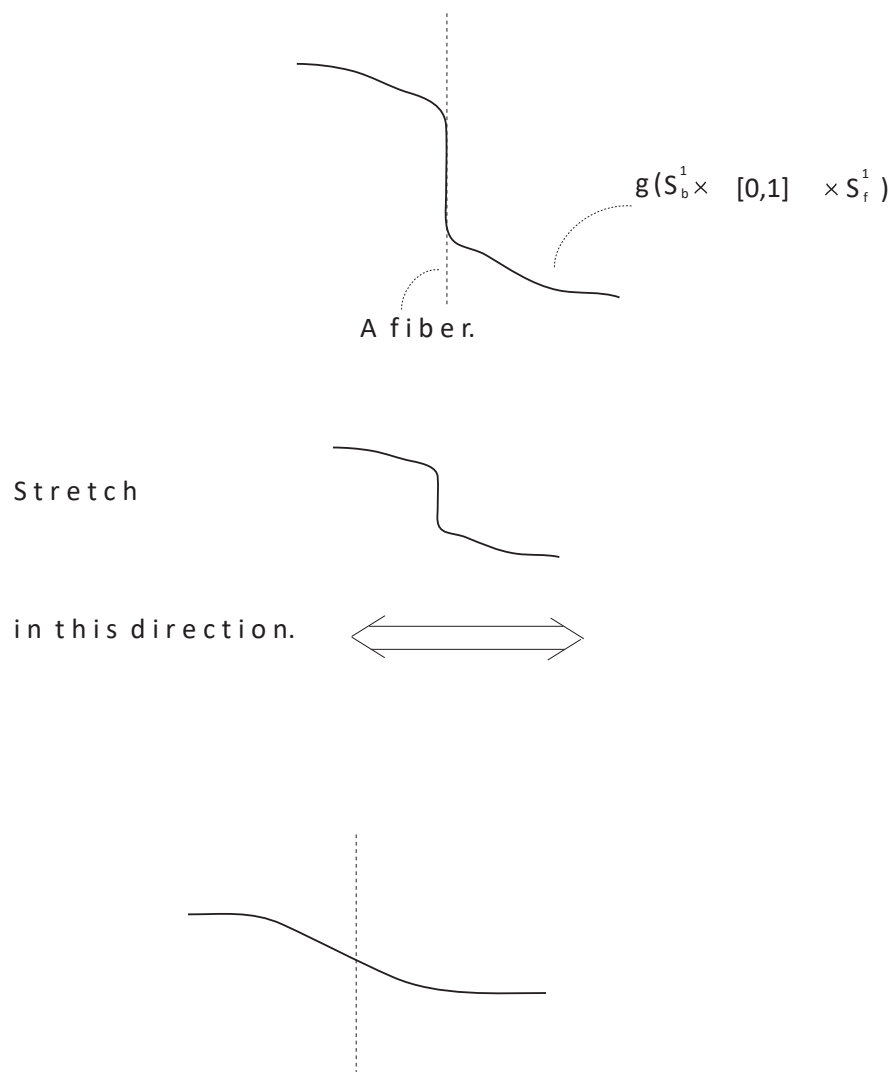


FIGURE 8.4. **The idea of how we stretch** $g(S_b^1 \times [0,1] \times S_f^1) \cap N$

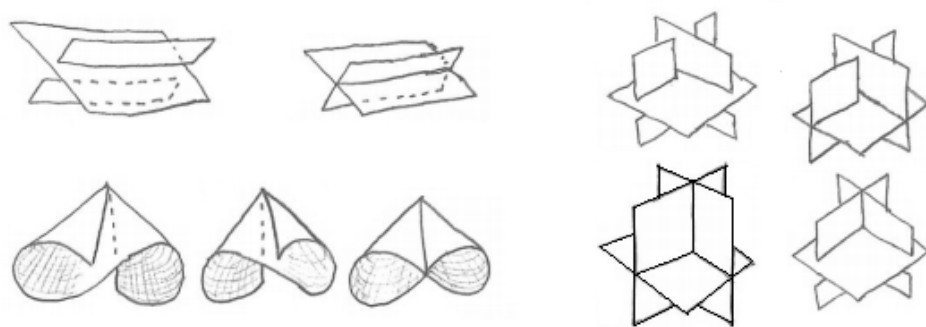


FIGURE 8.5. The singular point sets of welded 2-knots

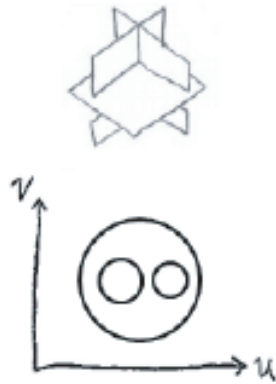


FIGURE 8.6. A new type of a nest of circles.

diagrams appearing throughout the process, then the diagrams are Welded equivalent and belong to the same Welded 2-knot type.

Note. The above definition makes sense both in the smooth and the PL category. The readers need not be familiar with Roseman moves in order to read this paper.

Note 8.16. When we consider circles in fiber \mathbb{R}^2 as in Note 8.14, there is a new type drawn in Figure 8.6, which is not in Figure 6.6.

Note 8.17. By Proposition 8.10, \underline{g} in Definition 8.12 satisfies the conditions (I)-(III) below, but \underline{g} is not generic.

(I) $\underline{g} : S_b^1 \times [0, 1] \rightarrow \mathbb{R}_b^2 \times [0, 1]$ is a continuous map such that $\underline{g}(S_b^1 \times \{t\}) \subset \mathbb{R}_b^2 \times \{t\}$ for any $t \in [0, 1]$.

(II) Let $t \in [0, 1]$. There are closed intervals, I_1, \dots, I_μ ($\mu \in \mathbb{N}$), such that $S_b^1 \times \{t\} = I_1 \cup \dots \cup I_\mu$ and such that $\underline{g}|_{I_i}$ is a PL embedding for each i .

(III) There are closed 2-discs, D_1^2, \dots, D_ν^2 ($\nu \in \mathbb{N}$), such that $S_b^1 \times [0, 1] = D_1^2 \cup \dots \cup D_\nu^2$ and such that $\underline{g}|_{D_i^2}$ is a PL embedding for each i .

Definition 8.18. If a map $\underline{g} : S_b^1 \times [0, 1] \rightarrow \mathbb{R}_b^2 \times [0, 1]$ satisfies the conditions (I)-(III) in Note 8.17, then \underline{g} is said to be *level preserving*. If \underline{g}' is obtained by moving \underline{g} by a homotopy \underline{G}_t , where $0 \leq t \leq 1$, $\underline{G}_0 = \underline{g}$ and $\underline{G}_1 = \underline{g}'$, keeping the conditions (I)-(III) of in Note 8.17, then we say that \underline{g}' is *level preserving homotopic* to \underline{g} or that we *perturb \underline{g} in the special way* and obtain \underline{g}' . We write $\underline{g} \sim \underline{g}'$. \underline{G}_t is called a *level preserving homotopy* or a *special homotopy*. Let $g : S_b^1 \times [0, 1] \times S_f^1 \rightarrow \mathbb{R}_b^2 \times [0, 1] \times \mathbb{R}_f^2$ be a map in Definition 8.12. Take a special homotopy \underline{G}_t of \underline{g} , and a special isotopy G_t of g where $0 \leq t \leq 1$. If \underline{G}_t is covered by G_t for any element t in $\{t | 0 \leq t \leq 1\}$, then we say that \underline{G}_t is *covered* by G_t .

Definition 8.19. Add the following condition to Definition 8.12 without changing the other parts. (8.19.1) We can perturb g in Definition 8.12 in the special way so that g covers a PL level preserving, generic map $S_b^1 \times [0, 1] \rightarrow \mathbb{R}_b^2 \times [0, 1]$.

We prove the following theorem.

Theorem 8.20. *Definition 8.19 is equivalent to Definition 8.12 (and, by Theorem 8.13, is equivalent to Definition 8.6.)*

Note 8.21. Even if we perturb $\underline{g} : S_b^1 \times [0, 1] \rightarrow \mathbb{R}_b^2 \times [0, 1]$, which is covered by g , in the special way by a special homotopy \underline{G}_t , \underline{G}_t is not covered by a special isotopy G_t of g in general. We must make \underline{G}_t under the condition that \underline{G}_t is covered by G_t .

Proof of Theorem 8.20. It is trivial that if g satisfies Definition 8.19, then g satisfies Definition 8.12. We prove the following.

Claim 8.22. *If g satisfies Definition 8.12, we can perturb g so that g satisfies Definition 8.19.*

Note. Recall that $\pi \circ g$ does not cover a generic map \underline{g} in general.

Proof of Claim 8.22.

The first step. Recall that by Definition 8.12, for each $t \in [0, 1]$, $(\text{Im}(\pi \circ g)) \cap (\mathbb{R}^2 \times \{t\})$ is an immersed circle. We prove the following.

Claim 8.23. *We can perturb g in the special way so that the singular point set of $(\text{Im}(\pi \circ g)) \cap (\mathbb{R}^2 \times \{t\})$ is a finite number of points except for a finite number of levels $t \in [0, 1]$. In other words, we can do so that for only a finite number of levels $t \in [0, 1]$, the singular point set of $(\text{Im}(\pi \circ g)) \cap (\mathbb{R}^2 \times \{t\})$ includes a finite number of segments.*

Proof of Claim 8.23. Let I denote the interior of a 1-simplex which is in a simplicial complex structure of the singular point set of $(\text{Im}(\pi \circ g)) \cap (\mathbb{R}^2 \times \{\gamma\})$ for a real number $\gamma \in [0, 1]$. Assume that I consists of multiple PL points.

Suppose that there are real numbers $\alpha, \beta \in [0, 1]$ with the following properties: $\alpha < \gamma < \beta$. For $\alpha < t < \beta$, $h_t : \mathbb{R}_b^2 \times \{\gamma\} \rightarrow \mathbb{R}_b^2 \times (\alpha, \beta)$ is an isotopy (t runs in (α, β)) such that $h_t((\text{Im}(\pi \circ g)) \cap (\mathbb{R}^2 \times \{\gamma\})) = (\text{Im}(\pi \circ g)) \cap (\mathbb{R}^2 \times \{t\})$ for all $t \in (\alpha, \beta)$, and such that h_t preserves the information of fiber-circles over two immersed circles which are put in the both sides of $=$. (Here, the information of fiber-circles means what we define in Theorem 4.3, Definition 4.4, Note 6.5, and Definition 6.6.) Note that $(g)^{-1}(I)$ is a disjoint union of n open segments I_1, \dots, I_n in $S_b^1 \times [0, 1]$. Note that $\bigcup_{\alpha < t < \beta} h_t(I)$ consists of n -tuple points, is an open set, and is a discrete submanifold of $\mathbb{R}_b^2 \times [0, 1]$. We can perturb g in the special way so that $\bigcup_{\alpha < t < \beta} h_t(I)$ separates n copies of $\bigcup_{\alpha < t < \beta} h_t(I)$ and so that we keep the boundary of the closure of $\bigcup_{\alpha < t < \beta} h_t(I)$ since there does not appear a new singularity of the immersed annulus. Figure 8.7 is an example.

Note 8.24. Figures 8.7-8.15 draw ‘figures in PL category’ although the figures are smoothened. When we move a map by isotopy, we take a PL subdivision if necessary.

Note that the boundary of the closure of each I may have a singular point set. The repetition of this procedure and Proposition 8.10 imply Claim 8.23. \square

Note 8.25. Note each point in the resultant part which is made from $\bigcup_{\alpha < t < \beta} h_t(I)$ by the separation. By the definition of I , it is a single point.

The second step. We prove the following.

Claim 8.26. *Suppose that g satisfies the condition of Claim 8.23. We can perturb g in the special way so that $\pi \circ g$ covers a level preserving transverse immersion \underline{g} except for a finite number of points contained in $S_b^1 \times [0, 1]$ with the following property: Let P be an exceptional point. Then $\underline{g}^{-1}(\underline{g}(P))$ may be more than one point.*

Proof of Claim 8.26. Since g satisfies the condition of Claim 8.23, the singular point set of $\text{Im}(\pi \circ g)$ is a 1-dimensional finite simplicial complex. Recall Proposition 8.10 and Note 8.25. Take the interior I of a 1-simplex in the singular point set of the simplicial complex structure with the following property:

- (1) $\underline{g}^{-1}(I)$ is disjoint n open segments I_1, \dots, I_n in $S_b^1 \times [0, 1]$ ($n \in \mathbb{N}$). $\underline{g}|_{I_i}$ is an embedding map.
- (2) There is an open neighborhood U of I in $\mathbb{R}_b^2 \times [0, 1]$ with the following property: There are open discs D_i^2 embedded in $S_b^1 \times [0, 1]$ each of which is a tubular neighborhood

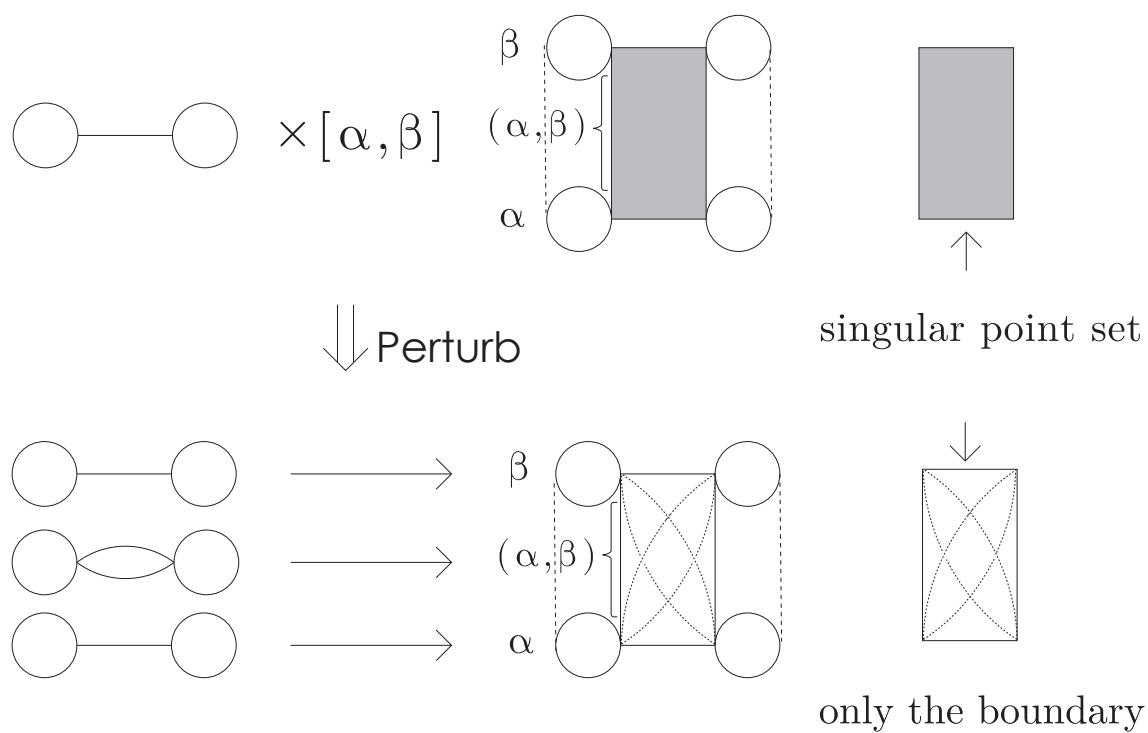


FIGURE 8.7. An example of fiberwise isotopy.

of I_i in $S_b^1 \times [0, 1]$ for each i . $D_i^2 \cap D_j^2 = \emptyset$ for each distinct i, j . $\underline{g}|_{D_i^2}$ is an embedding map. $U \cap \underline{g}(S_b^1 \times [0, 1])$ is $\underline{g}(D_1^2) \cup \dots \cup \underline{g}(D_n^2)$. $\underline{g}(D_i^2) \cap \underline{g}(D_j^2) = I$ for each distinct i, j .

We perturb $\underline{g}|_{(D_1^2 \cup \dots \cup D_n^2) \cap (\underline{g}^{-1}(U))}$ in the special way below but we must remember Note 8.21.

Let V be an open neighborhood of U in $\mathbb{R}_b^2 \times [0, 1]$. Hence $\overline{U} \subset V$.

Let $\wp : \mathbb{R}_b^2 \times [0, 1] \times \mathbb{R}_f^2 \rightarrow \mathbb{R}_f^2$. Combine this map \wp and the diagram in Note 8.3:

$$\begin{array}{ccccc} S_b^1 \times [0, 1] \times S_f^1 & \xrightarrow{g} & \mathbb{R}_b^2 \times [0, 1] \times \mathbb{R}_f^2 & \xrightarrow{\wp} & \mathbb{R}_f^2 \\ \downarrow \rho & \circlearrowleft & \downarrow \pi & & \\ S_b^1 \times [0, 1] & \xrightarrow{g} & \mathbb{R}_b^2 \times [0, 1] & & \end{array}$$

Claim 8.27. *We can perturb g in the special way, keeping out V (not U), with the following properties: The image $\wp(g(\rho^{-1}(D_i^2)))$ is a circle C_i . We have $C_i \cap C_j = \emptyset$ for each distinct i, j . The map $\wp|_{g(\rho^{-1}(D_i^2))}$ is the projection.*

Proof of Claim 8.27. Take a point $\sigma \in I$. Let $\underline{g}^{-1}(\sigma) = \{\sigma_1, \dots, \sigma_n\}$ and $\sigma_i \in I_i$. Then the image of $\wp(g(\rho^{-1}(\sigma_i)))$ is a circle C'_i , and we have $C'_i \cap C'_j = \emptyset$ for each distinct i, j . We can take g so that the circle C_i which we want is this circle C'_i for each i . Then Claim 8.27 holds. \square

Note. The reason why we prepare V is as follows: Before the perturbation, the map $\wp|_{g(\rho^{-1}(\partial D_i^2))}$ is not a projection. Note $\partial D_i^2 \subset \overline{U}$. However $\wp|_{g(\rho^{-1}(\partial D_i^2))}$ is the projection after the perturbation.

We next make $\underline{g}|_{(D_1^2 \cup \dots \cup D_n^2) \cap (\underline{g}^{-1}(U))}$ a level preserving transverse immersion since we can perturb g in the special way, keeping out U , with the following properties: For any point $q \in D_i^2$ and any point r in the circle $\rho^{-1}(q)$, $\wp(g(r)) \in \mathbb{R}_f^2$ is fixed while we perturb g . Claim 8.27 ensures that while we perturb g in this way, we keep a property that g is an embedding map. Figure 8.8 is an example of this procedure. The repetition of this procedure implies Claim 8.26. \square

The third step. We prove the following.

Claim 8.28. *Suppose that g satisfies the condition of Claim 8.26. We can perturb g in the special way so that $\pi \circ g$ covers a level preserving transverse immersion \underline{g} except for a finite number of points contained in $S_b^1 \times [0, 1]$ with the following property: Let P be any exceptional point. The set $\underline{g}^{-1}(\underline{g}(P))$ consists of only one point.*

Proof of Claim 8.28. Assume that $f^{-1}(f(P))$ consists of m points P_1, \dots, P_m ($m \in \mathbb{N}$) in $S_b^1 \times [0, 1]$. Take an open neighborhood U of $f(P)$ in $\mathbb{R}_b^2 \times [0, 1]$ with the following properties: There are open discs D_i^2 in $S_b^1 \times [0, 1]$ which is a tubular neighborhood of P_i in $S_b^1 \times [0, 1]$ for each i . $D_i^2 \cap D_j^2 = \emptyset$ for each distinct i, j . $U \cap \underline{g}(S_b^1 \times [0, 1])$

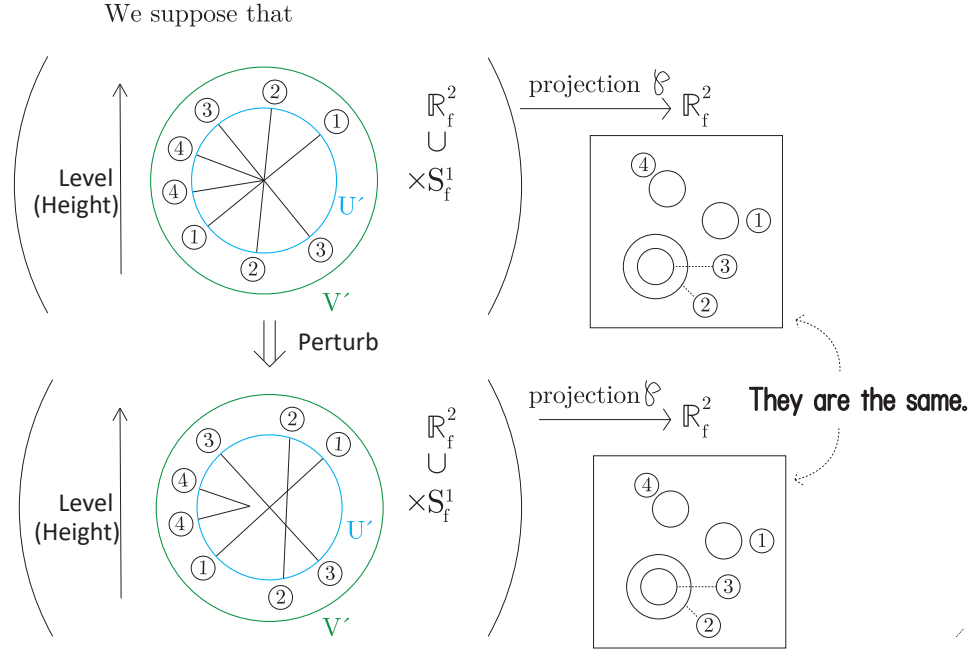


FIGURE 8.8. A special isotopy of g . The intersection of four sheets in the upper figure is perturbed and is changed into the one in the lower figure.

is $\underline{g}(D_1^2) \cup \dots \cup \underline{g}(D_m^2)$. $\underline{g}(D_1^2) \cap \dots \cap \underline{g}(D_m^2) = f(P)$. For a pair (i, j) , we may have $\underline{g}(D_i^2) \cap \underline{g}(D_j^2) \supsetneq f(P)$.

We perturb $\underline{g}|_{(D_1^2 \cup \dots \cup D_n^2) \cap (\underline{g}^{-1}(U))}$ in the special way below but we must remember Note 8.21. Take an open neighborhood V of U in $\mathbb{R}_b^2 \times [0, 1]$ such that $\overline{U} \subset V$. We can perturb \underline{g} in the special way, keeping out V (not U), with the following properties: $\wp(\underline{g}(\rho^{-1}(D_i^2)))$ is a circle C_i . $\wp|_{\underline{g}(\rho^{-1}(D_i^2))}$ is the projection.

We can make $\underline{g}|_{(D_1^2 \cup \dots \cup D_n^2) \cap (\underline{g}^{-1}(U))}$ a level preserving transverse immersion except for a finite number of points since we can perturb \underline{g} in the special way, keeping out U , with the following properties: For any point $q \in D_i^2$ and any point r in the circle $\rho^{-1}(q)$, $\wp(\underline{g}(r)) \in \mathbb{R}_f^2$ is fixed while we perturb \underline{g} . (Note that while we perturb \underline{g} in this way, we keep a property that \underline{g} is an embedding map.) The repetition of this procedure and Note 8.25 imply Claim 8.28. \square

The fourth step. Take $\pi \circ \underline{g}$ and \underline{g} in Claim 8.28. Let P be any exceptional point. Recall that $P \in S_b^1 \times [0, 1]$. Let $N(P)$ be the tubular neighborhood of P in $S_b^1 \times [0, 1]$. Take the tubular neighborhood B of $\underline{g}(P)$ in $\mathbb{R}_b^2 \times [0, 1]$. We can suppose that $\underline{g}(N(P)) \subset B$ and that $\underline{g}(\partial N(P)) \subset \partial B$. The image $\underline{g}(N(P))$ makes $\underline{g}(P)$ a branch point (recall Definition 6.1). Here we ignore the information of fiber circles over P . The information of Rourke fiber makes $\underline{g}(\partial N(P)) \subset \partial B$, a virtual 1-knot diagram ω in ∂B —(a point). Note that ∂B —(a point) is the 2-space and that the point is not included in ω . Recall virtual segments defined in Note 6.21. A *classical segment* is the segment with the following properties. It is a segment included in a virtual 2-knot diagram. One of the boundary is a classical branch point. The points in the interior of the segment are classical double points. An example is drawn in Figure 6.4 if the branch point there is a classical branch point.

Claim 8.29. *We can assume that all branch points of $\text{Im } \underline{g}$ are classical Whitney branch points.*

Proof of Claim 8.29. Since $\underline{g}(P)$ is a branch point, n virtual segments and m classical segments meet at $\underline{g}(P)$, where $\{n, m\} \subset \mathbb{N} \cup \{0\}$ and $n + m \geq 2$. We can prove that there is no virtual segment in the same fashion as the one in the proof of Theorem 6.23. (Note that in §6 we proved Theorem 6.23 in the smooth category but we can prove the PL version of Theorem 6.23 in the same way.) Therefore more than one classical segment meet at $\underline{g}(P)$. Hence ω is a classical diagram and determines a classical 1-knot.

In order to complete the proof of Claim 8.29, we will prove Claim 8.34. In order to prove Claim 8.34, we prove the following Claim 8.31.

Definition 8.30. Let $u, v \in [0, 1]$. Let $u \leq t \leq v$. The map $\underline{g}|_{S_b^1 \times [u, v]}$ is called a *product map* if there is an isotopy ι_t of \mathbb{R}^2 from the identity map such that $\iota_t : \mathbb{R}^2 \times \{u\} \rightarrow \mathbb{R}^2 \times \{t\}$ carries $(\text{Im } \underline{g}) \cap (\mathbb{R}^2 \times \{u\})$ to $(\text{Im } \underline{g}) \cap (\mathbb{R}^2 \times \{t\})$. Let B^3 be an embedded closed 3-ball in $\mathbb{R}_b^2 \times [0, 1]$. The map $\underline{g}|_{S_b^1 \times [u, v]}$ is called a *product map out B^3* if there is an isotopy ι_t of \mathbb{R}^2 from the identity map such that $\iota_t : \mathbb{R}^2 \times \{u\} \rightarrow \mathbb{R}^2 \times \{t\}$ carries $(\text{Im } \underline{g} - B^3) \cap (\mathbb{R}^2 \times \{u\})$ to $(\text{Im } \underline{g} - B^3) \cap (\mathbb{R}^2 \times \{t\})$.

We have the following.

Claim 8.31. *By using a special isotopy of g , any branch point is moved as drawn in Figure 8.9: Let α_u (respectively, α_v) be an immersed circle determined by $\underline{g}(S_b^1 \times \{u\}) \subset \mathbb{R}_b^2 \times \{u\}$ (respectively, $\underline{g}(S_b^1 \times \{v\}) \subset \mathbb{R}_b^2 \times \{v\}$) with the information of Rourke fiber determined by $\underline{g}(S_b^1 \times \{u\} \times S_f^1) \subset \mathbb{R}_b^2 \times \{u\} \times \mathbb{R}_f^2$ (respectively, $\underline{g}(S_b^1 \times \{v\} \times S_f^1) \subset \mathbb{R}_b^2 \times \{v\} \times \mathbb{R}_f^2$). The map $\underline{g}|_{S_b^1 \times [u, v]}$ is a product map out B . Hence $\alpha_u = \alpha_v \# \omega$, where $\#$ denotes the connected sum of immersed circles into \mathbb{R}^2 and $=$ means that there is an orientation preserving diffeomorphism of \mathbb{R}^2 which carries the left hand side to the right side one.*

Proof of Claim 8.31. For each t , $(\mathbb{R}_b^2 \times \{t\}) \cap \text{Im } \underline{g}$ is connected. Hence the branch point is not a local maximal (respectively, minimal) point of the restriction of the height function $\mathbb{R}_b^2 \times [0, 1] \rightarrow [0, 1]$ to $\text{Im } \underline{g}$.

Claim 8.32 follows from Claim 8.33.

Claim 8.32. *Let X be the closed interval contained in \mathcal{S} . Assume that X does not have self-intersection. Then, by using a special isotopy of g , we can move $\text{Int } X$ as drawn in Figure 8.10 with the following properties: We move $\text{Int } X$ by an isotopy of embedding of $\text{Int } X$, keeping the position of ∂X in $\mathbb{R}_b^2 \times [0, 1]$. We keep the position of $\overline{\mathcal{S} - X}$ in $\mathbb{R}_b^2 \times [0, 1]$. We keep the condition $X \cap (\mathcal{S} - X) = \emptyset$.*

In Figure 8.11 there is an example of Claim 8.32. There is drawn how X changes by a special isotopy of g in the case of the upper two figures in the right column of Figure 8.10. Note that $\text{Int } X$ consists of double points. Each point of ∂X is a branch, double or triple one. Let B be an open disc contained in $S_b^1 \times [0, 1] \times S_f^1$. By Definition 8.6.(1), $\pi \circ g(B)$ is not parallel to $\mathbb{R}_b^2 \times \{0\}$. Note that if $\pi \circ g(B)$ is parallel to $\mathbb{R}_b^2 \times \{0\}$, the phenomenon in the right column of Figure 8.11 does not occur.

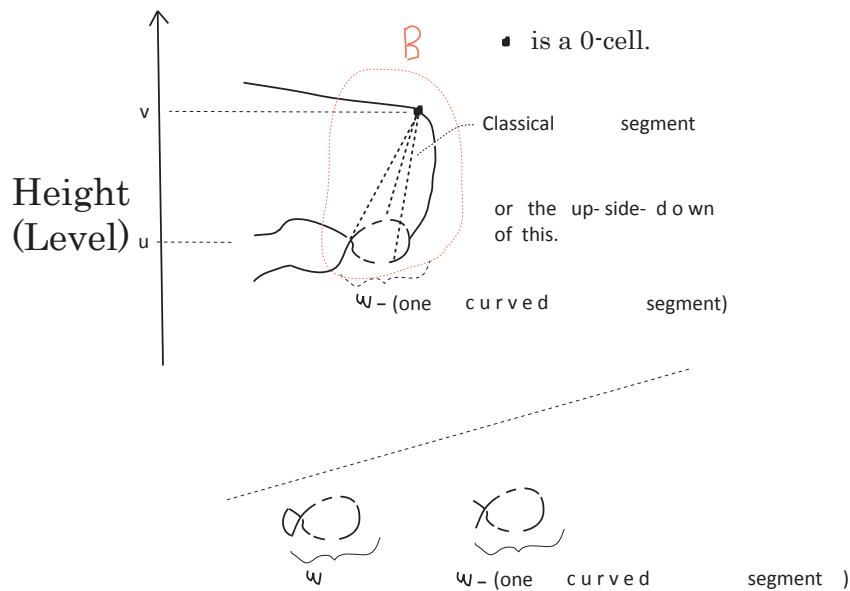


FIGURE 8.9. A branch point moved by a special isotopy of g

Claim 8.33. Let B^3 be a closed (respectively, open) 3-ball embedded in $R_b^2 \times [0, 1]$. Take any orientation preserving isotopy of diffeomorphism of B^3 fixing ∂B^3 from the identity map. We can give a coordinate (x, y, t) to $p \in B^3 \subset \mathbb{R}_b^2 \times [0, 1]$. Suppose that this isotopy carries p to a point whose coordinate is (x, y, t') , where $t' \neq t$ or $t' = t$ holds. Use this

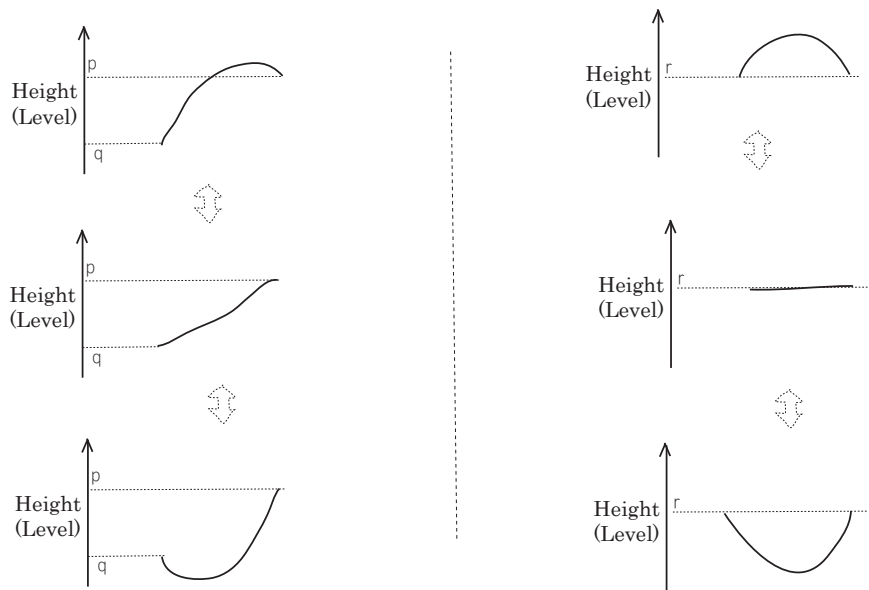


FIGURE 8.10. **Changing X .**

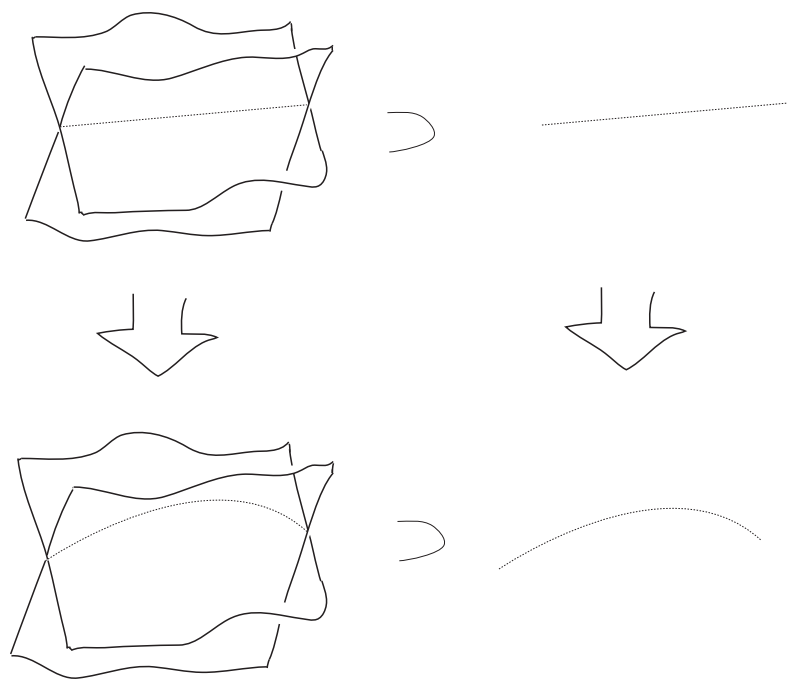


FIGURE 8.11. While the middle part of two sheets approaches by a special isotopy of g , the intersection X in Lemma 8.32 changes.

isotopy and make a homotopy of \underline{g} . Suppose that this homotopy is a special homotopy of \underline{g} . Then this homotopy of \underline{g} can be covered by a special isotopy of g .

By Claim 8.32, we can let the interior of all classical segments exist below (respectively, over) the branch point with respect to the height as drawn in Figure 8.9.

By the first, second and third steps, the singular point set of $\text{Im } \underline{g}$ is a finite simplicial complex. Hence we have the following.

Claim 8.34. *There are only finite number of $t \in [0, 1]$ with the following properties: There is no real number ε such that the map $\underline{g}|_{S_b^1 \times [t-\varepsilon, t+\varepsilon]}$ is a product map out B .*

By Claims 8.33 and 8.34, we have Claim 8.31. □

Claim 8.35. *ω defines the trivial knot. Hence we obtain α_v from α_u by using only classical Reidemeister moves.*

Proof of Claim 8.35. By the map $g|_{S_b^1 \times [u, v] \times S_f^1}$, α_u and α_v are fiberwise equivalent. Therefore the submanifolds, $\mathcal{S}(\alpha_u)$ and $\mathcal{S}(\alpha_v)$, of \mathbb{R}^4 are isotopic. Hence $\pi_1(\mathbb{R}^4 - \mathcal{S}(\alpha_u)) \cong \pi_1(\mathbb{R}^4 - \mathcal{S}(\alpha_v))$. Hence the group of α_u and that of α_v are isomorphic. Since $\alpha_u = \alpha_v \# \omega$, the group of α_u is the free product of that of α_v and that of ω . Hence the group of ω is \mathbb{Z} . Since ω defines a classical 1-knot, ω defines the trivial 1-knot. Since ω is a classical 1-knot diagram and represents the trivial 1-knot, ω is changed into the trivial 1-knot diagram by using only classical Reidemeister moves. Hence Claim 8.35 holds. □

It is easy to prove that if two virtual 1-knot diagrams are obtained each other by using only classical Reidemeister moves, they are fiberwise equivalent. Therefore, we change $\underline{g}|_{S_b^1 \times [u, v]}$ in B so that we let the map $\underline{g}|_{S_b^1 \times [u, v]}$ be a level preserving, generic map. Hence the following holds: If $\underline{g}(S_b^1 \times [u, v])$ includes a branch point, it is the classical Whitney branch point. These classical Whitney branch points appear when we carry out classical Reidemeister I move while we change α_u into α_v . After repeating this procedure, all branch points of $\text{Im } \underline{g}$ are classical Whitney branch points. This completes the proof of Claim 8.29. □

This completes the proof of Claim 8.22. □

This completes the proof of Theorem 8.20. □

Claim 8.35 implies the following Proposition 8.37.

Definition 8.36. Virtual 1-knot diagrams α and β are said to be *strongly fiberwise equivalent* if α and β satisfy the conditions which are made by replacing the phrase ‘level

preserving generic map' with 'level preserving transverse immersion' without changing other parts in Definition 8.19.

Proposition 8.37. *If virtual 1-knot diagrams α and β are fiberwise equivalent, there is a sequence of virtual 1-knot diagrams, $\alpha = \alpha_1, \beta_1, \alpha_2, \beta_2, \dots, \alpha_{k-1}, \beta_{k-1}, \alpha_k, \beta_k = \beta$ ($k \in \mathbb{N}$), such that α_i and β_i are strongly fiberwise equivalent ($1 \leq i \leq k$) and such that β_i and α_{i+1} ($1 \leq i \leq k-1$) are classical move equivalent (and therefore rotational welded equivalent).*

We prove the following theorem.

Theorem 8.38. *If g satisfies Definition 8.36, then the following hold. Let \mathcal{S} be the singular point set of $(\pi \circ g)(S_b^1 \times [0, 1] \times S_f^1)$ in Definition 8.36. Note that \mathcal{S} is a finite 1-dimensional simplicial complex.*

- (i) $\mathcal{S} \cap (\mathbb{R}_b^2 \times \{0 \text{ (respectively, } 1)\})$ is a set of virtual and classical crossing points of α (respectively, β), and therefore is a set of double points. It consists of 0-simplices. Only one 1-simplex is attached to each of these 0-simplices. These 1-simplices meet $\mathbb{R}_b^2 \times \{0 \text{ (respectively, } 1)\}$ transversely.
- (ii) Triple points are 0-simplices. (Recall Notes 8.14 and 8.16, Definition 8.15.)
- (iii) The restriction of 'the height function $\mathfrak{h} : \mathbb{R}_b^2 \times [0, 1] \rightarrow [0, 1]$ ' to the interior of any 1-simplex in \mathcal{S} has no critical point. (Hence we have the following: For each $\zeta \in [0, 1]$, $\mathcal{S} \cap (\mathbb{R}_b^2 \times \{\zeta\})$ is a finite number of points. No 1-simplex is parallel to $\mathbb{R}_b^2 \times \{0\}$.)
- (iv) Let $\zeta \in (0, 1)$. $\mathcal{S} \cap (\mathbb{R}_b^2 \times \{\zeta\})$ includes no or only one 0-simplex.
- (v) In $\mathbb{R}_b^2 \times (0, 1)$, 0-simplices appear only in the two cases of Figure 8.12.

Proof of Theorem 8.38. Theorem 8.38.(i) follows from Definition 8.36.(5) for any simplicial complex structure. Theorem 8.38.(ii) holds for any simplicial complex structure by the definition of simplicial complex structure.

Proof of Theorem 8.38.(iii). Suppose that there is an X as is an example explained in Claim 8.32 and Figure 8.11. Repeating this procedure we can take a simplicial complex structure such that $(\text{any 1-simplex}) \cap (\mathbb{R}_b^2 \times \{t\})$ for any $t \in [0, 1]$ is a finite number of points. Therefore the restriction of \mathfrak{h} to the interior of any 1-simplex of this simplicial complex structure has a finite number of critical points. Make a new simplicial complex structure so that the critical points are new 0-simplicies so that we keep the condition of Theorems 8.38.(i) and (ii). Suppose that there is a 0-simplex e^0 to which only two 1-simplices e_1^1 and e_2^1 , attach, and that e^0 is not a critical point of the restriction of \mathfrak{h} to $(\text{Int}e_1^1) \cup e^0 \cup (\text{Int}e_2^1) = \text{Int}(e_1^1 \cup e^0 \cup e_2^1)$. Make a new simplicial complex structure such that $e_1^1 \cup e^0 \cup e_2^1$ is changed into a new 1-simplex without changing other simplicial complex structure. This completes the proof of Theorem 8.38.(iii).

■ is a 0-cell.

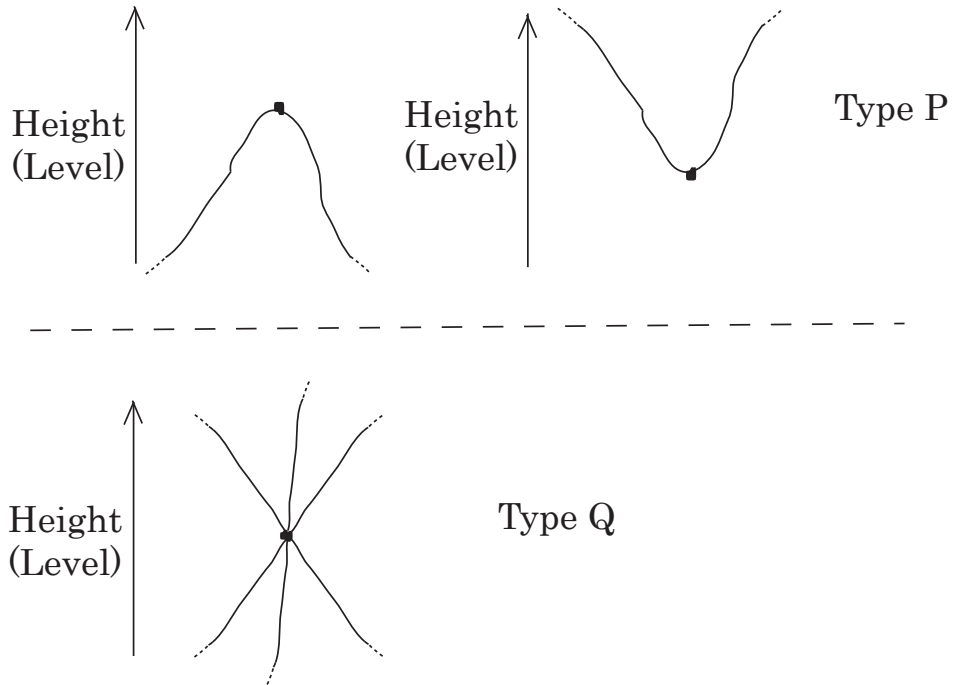


FIGURE 8.12. 0-simplices in \mathcal{S}

Theorem 8.38.(iv) holds because, by Claims 8.34 and 8.33, we can change the height of any 0-simplex so that we keep the condition of Theorems 8.38.(i)-(iii).

Proof of Theorem 8.38.(v). There are only two cases: (P) Only two 1-simplices attach to a 0-simplex. (Q) Only six 1-simplices attach to a 0-simplex. Note that, by Theorem 8.38.(iii), each 1-simplex is attached to two different 0-simplices. In the case (P), by Theorem 8.38.(iii), the 0-simplex exists as drawn in Type P of Figure 8.12. In the case (Q), as drawn in Figure 8.11 associated with Claim 8.32, we can move 1-simplex so that we have the condition as drawn in Type Q of Figure 8.12, and so that we keep the condition of Theorems 8.38.(i)-(iv). See Figure 8.13 for an example of this move.

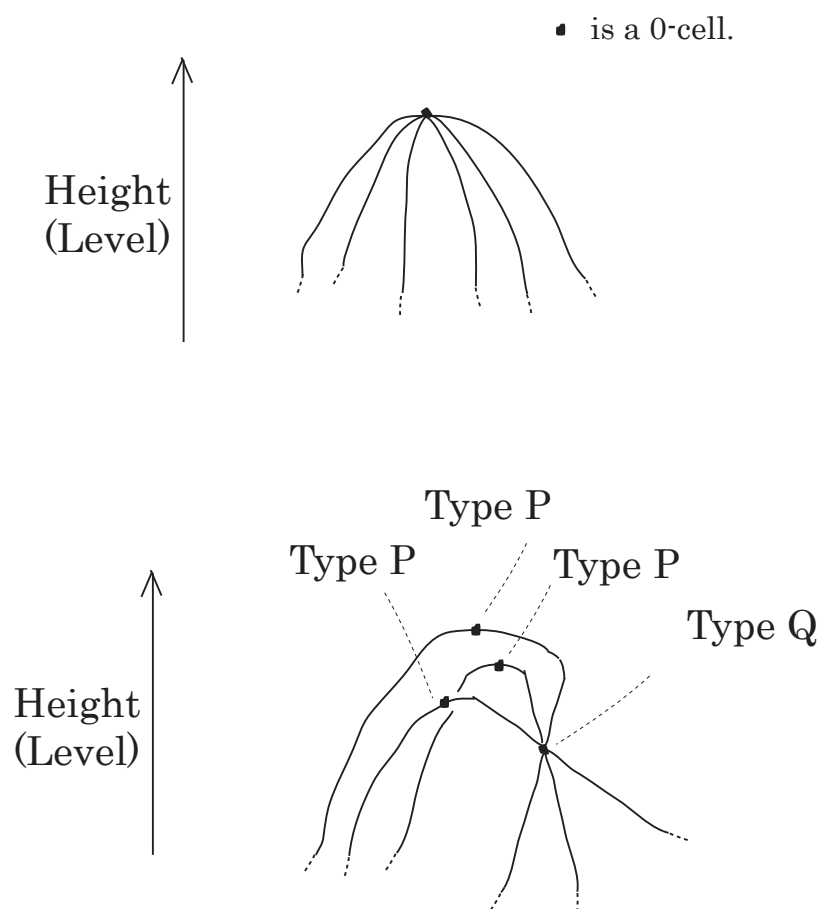


FIGURE 8.13. The singularity in the upper figure is made into the one in the lower which consists of one Type Q and three Type P.

This completes the proof of Theorem 8.38.(v).

This completes the proof of Theorem 8.38. □

We have the following theorem.

Theorem 8.39. *Two virtual 1-knot diagrams α and β are PL fiberwise equivalent if and only if α and β are PL rotational welded equivalent.*

Proof of Theorem 8.39. The ‘if’ part is easy.

We prove the ‘only if’ part. By Proposition 8.37, it suffices to prove Claim 8.40

Claim 8.40. *Two virtual 1-knot diagrams α and β are PL strongly fiberwise equivalent only if α and β are PL rotational welded equivalent.*

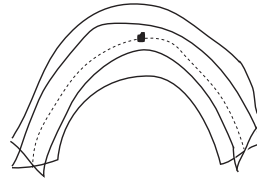
Proof of Claim 8.40. Let $C_\zeta = \underline{g}(S_b^1 \times \{\zeta\}) = \underline{g}(S_b^1 \times [0, 1]) \cap (\mathbb{R}_b^2 \times \{\zeta\})$
 $= (\pi \circ g(S_b^1 \times [0, 1] \times S_f^1)) \cap (\mathbb{R}_b^2 \times \{\zeta\})$. By Theorem 8.38, C_ζ is an immersed circle in $\mathbb{R}_b^2 \times \{\zeta\}$ and its singular point set is a finite number of points. C_ζ changes from α to β step by step as ζ runs from 0 to 1. If, for a ζ_p , C_{ζ_p} includes a 0-simplex of the simplicial complex structure in Theorem 8.38. A classical or virtual Reidemeister move is done there. We do any of them only there. If $\zeta_q < \zeta < \zeta_r$, C_ζ includes no 0-simplex. Then C_ζ is not changed while ζ runs from ζ_q to ζ_r . We investigate how C_ζ changes in detail. Near a 0-simplex in $\mathbb{R}_b^2 \times [0, 1]$, $\text{Im } \underline{g}$ is drawn as in Figure 8.14 since \underline{g} is a transverse immersion. Here, note that we can move \mathcal{S} by using a special isotopy of \bar{g} .

Therefore we have only the following two facts on \mathcal{S} and local moves on the knot diagrams.

(i) Let $\sigma, \tau \in [0, 1]$. Suppose that $\mathcal{S} \cap (\mathbb{R}_b^2 \times (\sigma, \tau))$ includes no 0-simplex. It holds that $\underline{g}|_{S_b^1 \times [\sigma, \tau]}$ is a product map. Then $(\pi \circ g)(S_b^1 \times [0, 1] \times S_f^1) \cap (\mathbb{R}_b^2 \times \{\sigma\})$ can be obtained from $(\pi \circ g)(S_b^1 \times [0, 1] \times S_f^1) \cap (\mathbb{R}_b^2 \times \{\tau\})$ by an isotopy of \mathbb{R}_b^2 .

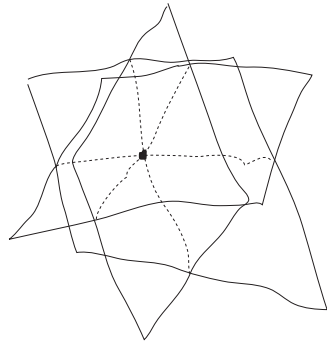
(ii) Let $\xi \in [0, 1]$. Suppose that $\mathcal{S} \cap (\mathbb{R}_b^2 \times \{\xi\})$ includes only one 0-simplex. Suppose that $\mathcal{S} \cap (\mathbb{R}_b^2 \times (\xi, \xi + \varepsilon])$ (respectively, $\mathcal{S} \cap (\mathbb{R}_b^2 \times [\xi - \varepsilon, \xi))$) includes no 0-simplex. Let $D = (\pi \circ g)(S_b^1 \times [0, 1] \times S_f^1) \cap (\mathbb{R}_b^2 \times \{\xi - \varepsilon'\})$ and $U = (\pi \circ g)(S_b^1 \times [0, 1] \times S_f^1) \cap (\mathbb{R}_b^2 \times \{\xi + \varepsilon'\})$. If the 0-simplex is put in Type P or Q, then U is obtained from D by one welded move other than a virtual Reidemeister I move. (Note. Type P causes classical and virtual Reidemeister II moves. Type Q causes classical and virtual Reidemeister III moves. Four types of triple points correspond to four types of classical and virtual Reidemeister III moves.) Therefore α is changed into β by welded moves other than the virtual Reidemeister I move. Hence α is rotational

• is a 0-cell.



and the up-side-down
of this.

Type P



Type Q

FIGURE 8.14. **How sheets intersect near Types P and Q.**

welded equivalent to β . This completes the proof of Claim 8.40. □

This completes the proof of Theorem 8.39. □

We will complete the proof of Theorem 8.5 and go back to the smooth category. We said that the ‘if’ part of Theorem 8.5 is easy. We will prove the ‘only if’ part of Theorem 8.5 by using the following lemma.

Lemma 8.41. *Let α and β be smooth virtual 1-knot diagrams. Let α' (respectively, β') be a PL virtual 1-knot diagram which is piecewise smooth, planar, ambient isotopic to α (respectively, β). Then we have the following. α and β are smooth rotational welded equivalent if and only if α' and β' are PL rotational welded equivalent.*

Proof of Lemma 8.41. Let ξ and ζ be smooth virtual 1-knot diagrams. If ξ and ζ are PL, planar, ambient isotopic to a PL virtual 1-knot diagram γ , then ξ is smooth, planar, ambient isotopic to ζ . *Reason.* Smoothen the corner of γ . Each of PL rotational welded Reidemeister moves is regarded as smooth rotational welded Reidemeister move. This completes the proof of Lemma 8.41. \square

Assume that two virtual 1-knot diagrams α and β are smooth fiberwise equivalent. By Claim 8.7, they are PL fiberwise equivalent. By Theorem 8.39, they are PL rotational welded equivalent. By Lemma 8.41, they are smooth rotational welded equivalent. Therefore the ‘only if’ part of Theorem 8.5 is true.

This completes the proof of Theorem 8.5. \square

We are now back to the smooth category.

Note. Figure 8.15 explains Figure 8.13 in more detail.

Note 8.42. In [38], the fiberwise equivalence is defined by the following definition. We call the equivalence relation the *f-fiberwise equivalence* in this paper. Note that we work in the smooth category.

Definition 8.43. Add the following condition to Definition 8.1 without changing the other parts. We call the equivalence relation the *f-fiberwise equivalence*. Note that we work in the smooth category.

(8.43.1) In each fiber \mathbb{R}_f^2 , there are a finite number of circles. (That is, $< \infty$.)

We said that it is easy to prove the following (i). It is also easy to prove the following (ii).

- (i) If virtual 1-knot diagrams α and β are rotational welded equivalent, then α and β are fiberwise equivalent.
- (ii) If virtual 1-knot diagrams α and β are rotational welded equivalent, then α and β are *f-fiberwise* equivalent.

Theorem 8.5 and the above (ii) imply the following (iii).

- (iii) If virtual 1-knot diagrams α and β are fiberwise equivalent, then α and β are *f-fiberwise* equivalent. (Note that we work in the smooth category.)

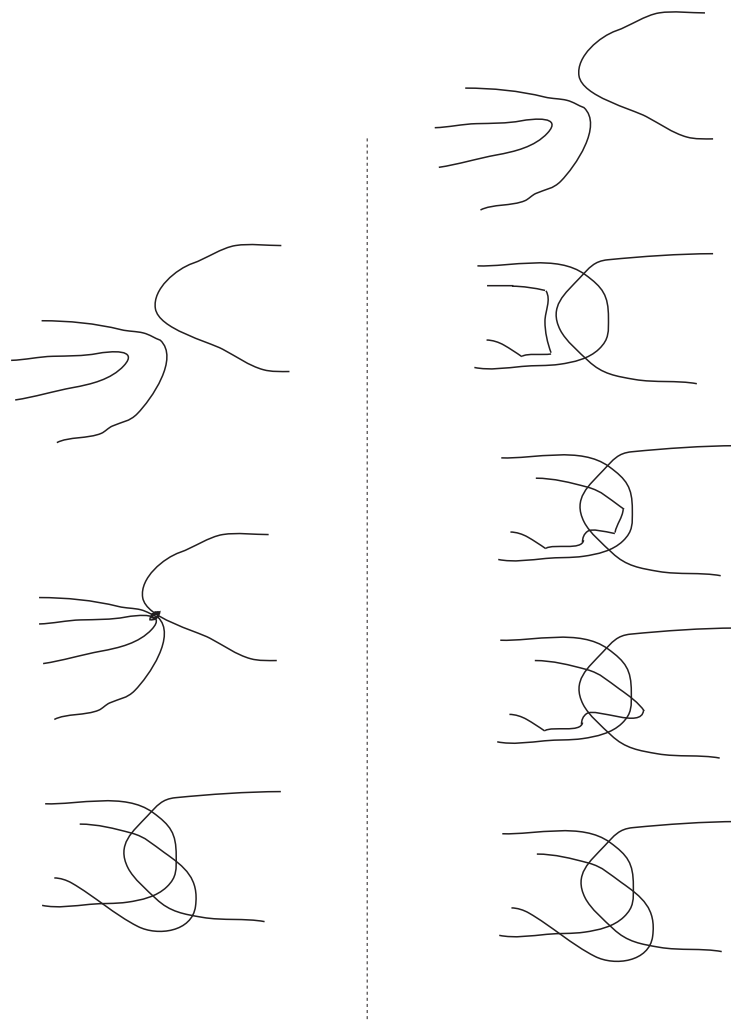


FIGURE 8.15. This pair of the left figure and the right one is an example of a pair of the figures of Figure 8.13. The left (respectively, right) figure is an example of a sequence of diagrams associated with the upper (respectively, lower) figure of Figure 8.13. The left sequence is perturbed and is made into the right sequence. These diagrams are drawn without information of virtual multiple points and classical ones.

The converse of (iii) is trivial. Hence we have the following: Virtual 1-knot diagrams α and β are fiberwise equivalent if and only if α and β are f -fiberwise equivalent

Note 8.44. Although Rourke claimed in [38, Theorem 4.1] that two virtual 1-knot diagrams α and β are fiberwise equivalent if and only if α and β are welded equivalent in the PL (respectively, smooth) category, we state that this claim is wrong, as we mentioned it in the last few paragraphs of §1.3. The reason for the wrongness is Theorems 8.5 and 8.39 and Claim 8.47.

We introduce a new equivalence relation of the set of virtual 1-knot diagrams.

Definition 8.45. Let α and β be virtual 1-knot diagrams. We say that α and β are *virtually parity equivalent* if α and β have the same parity of virtual crossing points.

We prove several results associated with the virtual parity.

Claim 8.46. *If two virtual 1-knot diagrams α and β are rotational welded equivalent, then α and β are virtually parity equivalent.*

Proof of Claim 8.46. We can obtain α from β by some welded-moves other than virtual Reidemeister I move. □

Claim 8.47. *The welded equivalence does not imply the rotational welded equivalence.*

Note. By their definitions, the rotational welded equivalence implies the welded equivalence.

Proof of Claim 8.47. Call the virtual 1-knot diagram in Figure 8.16, the *virtual figure ∞ knot diagram*.

The virtual figure ∞ knot diagram and the trivial 1-knot diagram are welded equivalent by the definition but are not rotational welded equivalent by Claim 8.46.

This completes the proof of Claim 8.47. □

8.2. Related topics.

Theorem 8.48 is one of our main results.

Theorem 8.48. *If two virtual 1-knot diagrams α and β are fiberwise equivalent, then α and β are virtually parity equivalent.*

Proof of Theorem 8.48. Theorem 8.5 and Claim 8.46 imply Theorem 8.48. □

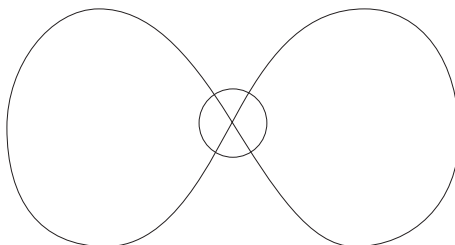


FIGURE 8.16. The virtual figure ∞ knot diagram

It is known that the usual trefoil knot diagram is not welded equivalent to the trivial knot diagram (see [16, 18, 38, 40, 41]). Hence these two diagrams are not also rotational welded equivalent. Hence we have the following.

Claim 8.49. *The converse of Theorem 8.48 is not true in general.*

We have the following.

Claim 8.50. *The number of virtual crossing points of virtual 1-knot diagrams is not an invariant of the fiberwise equivalence (respectively, the rotational welded equivalence) in general.*

Proof of Claim 8.50. The two virtual knot diagrams in Figure 8.17 are fiberwise equivalent (respectively, rotational welded equivalent). \square

We introduce a ‘weaker’ equivalence relation than the fiberwise equivalence defined by Definition 8.1. We want to replace ‘level preserving embedding of $S_b^1 \times [0, 1]$ ’ in Definition 8.1 with an oriented compact surface which is not necessarily ‘level preserving embedding of $S_b^1 \times [0, 1]$ ’, and loose a few conditions there. We prove in Theorem 8.52 that this equivalence relation is equivalent to the virtual parity equivalence relation.

Definition 8.51. Let α and β be virtual 1-knot diagrams. We say that α and β are *weakly fiberwise equivalent* if α and β satisfy the following conditions.

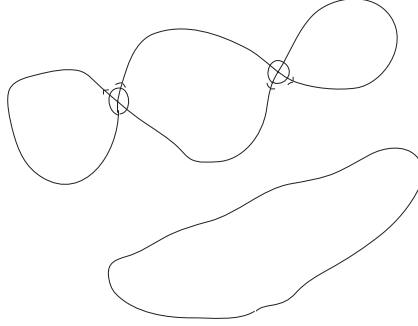


FIGURE 8.17. Two virtual knot diagrams which are rotational welded equivalent (respectively, fiberwise equivalent).

(1) There is a compact generic oriented surface F with boundary whose boundary is a disjoint union of two circles, which is contained in $\mathbb{R}_b^2 \times [0, 1]$, and F is covered by Rourke's fibration. Note that thus there is a submanifold of $\mathbb{R}_b^2 \times [0, 1] \times \mathbb{R}_f^2$ which is diffeomorphic to $F \times S^1$.

(2) The in-out information of fiber circles gives α and β the information whether each multiple (respectively, branch) point is virtual or classical as in Theorem 4.3.

(3) ∂F is α and β . F meets $\mathbb{R}_b^2 \times \{0\}$ (respectively, $\mathbb{R}_b^2 \times \{1\}$) at α (respectively, β) transversely.

If F above is an annulus, we say that α and β are *fiberwise cobordant*.

Theorem 8.52. *Let α and β be virtual 1-knot diagrams. α and β are weakly fiberwise equivalent if and only if α and β are virtually parity equivalent.*

Proof of Theorem 8.52. The ‘only if’ part: We use ‘reductio ad absurdum’. We suppose an assumption: α and β are not virtually parity equivalent. Take a generic surface which connects α and β as in Definition 8.51. Then this generic surface must have at

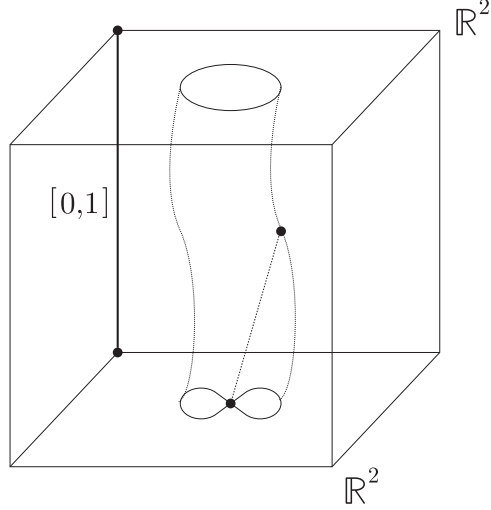


FIGURE 8.18. Let α be the virtual figure ∞ knot diagram and β , the trivial 1-knot diagram. For example, $(\pi \circ g)(S_b^1 \times [0, 1] \times S_f^1)$ cannot be realized as drawn above, by Theorem 6.23.

least one virtual branch point because the union of α and β has an odd number of virtual crossing point. By Theorem 6.23, this generic surface never exists. (See Figure 8.18.) We arrived at a contradiction. Hence the above assumption is false and the ‘only if’ part is true.

The ‘if’ part: It suffices to prove that $\alpha \amalg (-\beta)$ in \mathbb{R}^2 , where \amalg denote the disjoint union of the diagrams, is weakly fiberwise equivalent to the trivial 1-knot diagram. We can attach bands as drawn in Figure 8.19 so that the orientations of virtual knot diagrams and those of the bands are compatible. Thus $\alpha \amalg (-\beta)$ is weakly fiberwise equivalent to the disjoint union of nonnegative even integer of copies of the virtual figure ∞ knot and a classical link diagram. We can attach a band to two copies of the virtual figure ∞ knot diagram and combine them as drawn in Figure 8.20, so that the orientation of the band

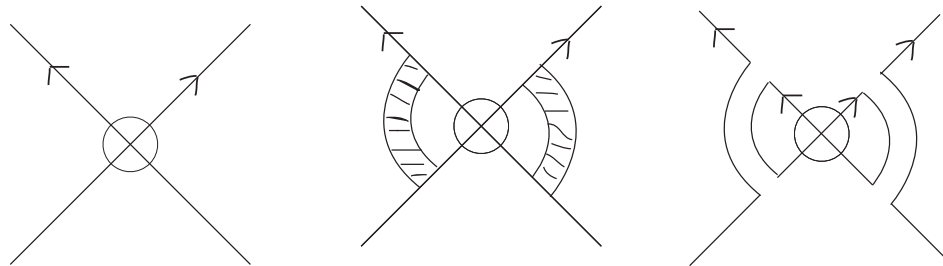


FIGURE 8.19. **Attaching bands.**

and those of the knot diagrams are compatible, and call the resultant diagram ζ . Thus $\alpha \amalg (-\beta)$ in \mathbb{R}^2 is weakly fiberwise equivalent to the disjoint union of a finite number of copies of ζ . It is easy to prove that ζ is rotational welded equivalent to the trivial knot. Suppose that we obtain the μ -component trivial 1-link diagram after that. Attach $\mu - 1$ copies of 2-disc to $(\mu - 1)$ components of this trivial 1-link diagram. Hence $\alpha \amalg (-\beta)$ is weakly fiberwise equivalent to the trivial 1-knot diagram. Hence α and β are weakly fiberwise equivalent. This completes the proof of Theorem 8.52. \square

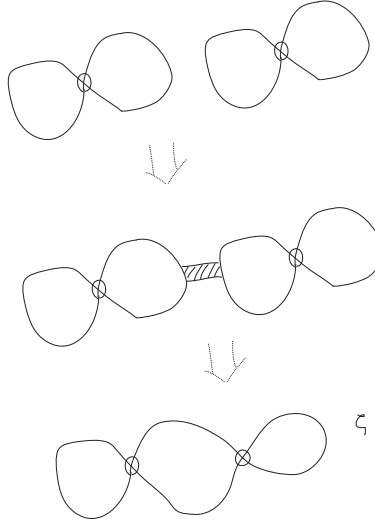


FIGURE 8.20. A combination of two copies of the virtual figure ∞ knot diagram

Definition 8.53. We define the ‘*nonorientably weakly fiberwise equivalence*’. In Definition 8.51 replace ‘oriented surface’ with ‘non-orientable surface’, and replace ‘weakly fiberwise equivalent’ with ‘nonorientably weakly fiberwise equivalent’.

Theorem 8.54. *Let α and β be virtual 1-knot diagrams. α and β are nonorientably weakly fiberwise equivalent if and only if α and β are virtually parity equivalent.*

Proof of Theorem 8.54. The ‘if’ part: By Theorem 8.52, α and β are weakly fiberwise equivalent. It is trivial that if α and β are weakly fiberwise equivalent, then α and β are nonorientably weakly fiberwise equivalent. *Reason.* Take a generic oriented surface for α and β as in Definition 8.51. Take an immersed Klein bottle in $\mathbb{R}_b^2 \times [0, 1]$. Connect the generic oriented surface and the immersed Klein bottle by using an embedded 3-dimensional 1-handle in \mathbb{R}^3 such that the intersection of the 1-handle and the oriented surface (respectively, immersed Klein bottle) is only the attaching part of the 1-handle. The resultant generic nonorientable surface implies that α and β are nonorientably weakly

fiberwise equivalent. The proof of the ‘only if’ part is the same as that of the ‘only if’ part of Theorem 8.52 if we replace the words ‘Definition 8.51’ with ‘Definition 8.53’, and remove the sentence ‘(See Figure 8.18.)’. \square

Define *Whitney degree* of any virtual 1-knot diagram α to be Whitney degree which is defined by α when we regard α as an immersed oriented circle in \mathbb{R}^2 . Two virtual 1-knot diagrams α and β are said to be *Whitney parity equivalent* if the parity of Whitney degree of α is the same as that of β . Two virtual 1-knot diagrams α and β are said to be *classically parity equivalent* if the parity of the classical crossing points of α is the same as that of β . The following holds. Let α and β be virtual 1-knot diagrams which are rotational welded equivalent (respectively, fiberwise equivalent). (Note Theorem 8.5.) Then α and β are classically parity equivalent if and only if α and β are Whitney parity equivalent.

Reason. α and β are Whitney parity equivalent if and only if the number of the classical Reidemeister I moves is even in a sequence of rotational welded moves which α is changed into β . Note that we cannot use the virtual Reidemeister I move by definition.

Some readers may ask the following question: Suppose that two virtual 1-knot diagrams α and β do not have any classical crossing point and that Whitney degrees are different. Then is it valid that α and β are not rotational welded equivalent? The answer is negative. We show a counter example in Figure 8.21.(i) (respectively, 8.21.(ii)). The proof that each pair is rotational welded equivalent is left to the reader.

Two virtual 1-knot diagrams α and β are said to be *mixed parity equivalent* if the parity of the sum of the classical and virtual crossing points of α is the same as that of β . The following holds. Let α and β be virtual 1-knot diagrams which are welded equivalent. Then α and β are mixed parity equivalent if and only if α and β are Whitney parity equivalent.

Reason. α and β are Whitney parity equivalent if and only if the sum of the number of the classical and virtual Reidemeister I moves is even in a sequence of welded moves which α is changed into β .

9. VIRTUAL HIGH DIMENSIONAL KNOTS

See [20, 21, 22, 28, 35] for codimension two high dimensional knots. See [6, 7, 27] for high codimensional high dimensional knots. It is natural to attempt to define virtual high dimensional knots and their one-dimensional-higher tubes. We could define n -dimensional virtual knots by using virtual n -knot diagrams in \mathbb{R}^{n+1} . We would make any virtual n -knot into a submanifold of (a closed oriented n -manifold M) $\times [0, 1]$ as we do in the virtual 1- and 2-dimensional cases. We want to make a bijection between the set of such

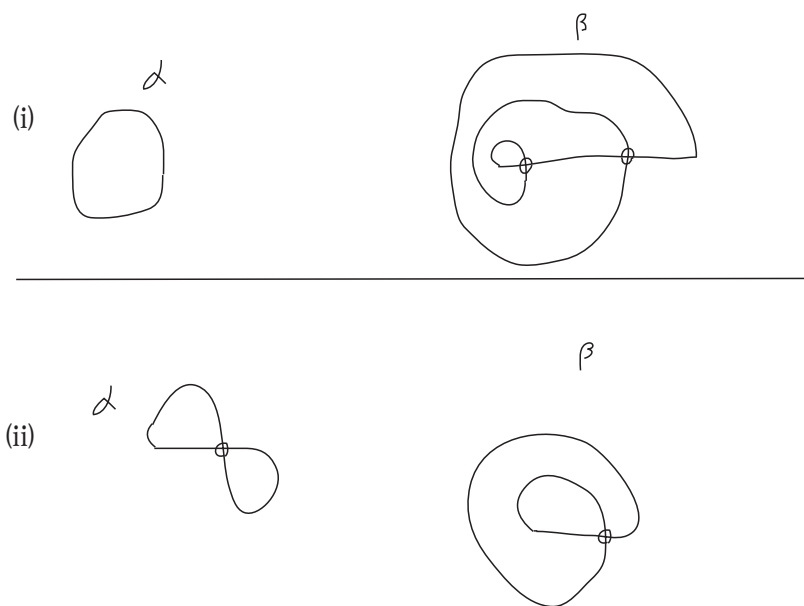


FIGURE 8.21. Two pairs of virtual knot diagrams

submanifolds and that of virtual n -knots. The 1-dimensional case is done (see Theorem 2.1 and Definition 6.9). We should define a one-dimensional-higher tube as the spinning submanifold made from K around M . Satoh's method makes no sense in the dimension greater than one. Rourke's way also makes non-sense by Theorem 6.23. Furthermore we must note that the n -dimensional case ($n \in \mathbb{N} - \{1, 2\}$) of Theorems 4.7 and 6.17 does not necessarily hold in smooth category (respectively, PL category) because it is not trivial to produce an analogue of their proof by the following fact of [10]: There is an integer $p \geq 3$ and are two smooth (respectively, PL) a -dimensional submanifolds, X and Y , of S^{a+p} which are diffeomorphic (respectively, PL homeomorphic) each other but which are non-isotopic as smooth submanifolds (respectively, PL submanifolds). To complete these topics in this section is left to the readers as problems.

REFERENCES

- [1] D. Bar-Natan: Balloons and hoops and their universal finite-type invariant, BF theory, and an ultimate Alexander invariant, *Acta Math. Vietnam.* 40 (2015) 271-329.
- [2] D. Bar-Natan and Z. Dansco: Finite-type invariants of w-knotted objects, I: w-knots and the Alexander polynomial: *Algebr. Geom. Topol.* 16 (2016) 1063-1133.
- [3] W. Boy: Über die Curvatura integra und die Topologie geschlossener Flächen, *Math. Ann.* 57 (1903) 151-184.
- [4] G. Burde and H. Zieschang: Knots, De Gruyter, *Studies in Math.* no.5 De Gruyter (1985).
- [5] L. Crane: 2-d physics and 3-d topology. *Comm. Math. Phys.* 135 (1991), no. 3, 615-640.
- [6] A. Haefliger: Knotted $(4k-1)$ spheres in $6k$ space *Annals of Math.* 75 (1962) 452-466.
- [7] A. Haefliger: Differentiable embeddings of S^n in S^{n+q} for $q > 2$ *Annals of Math* 83 (1966) 402-436.
- [8] A. Haefliger: Differentiable imbeddings *Bull. Amer. Math. Soc.* 67 (1961) 109-112.
- [9] W. Hirsch: The imbedding of bounding manifolds in euclidean space *Ann. of Math* 74 (1961), 494-497.
- [10] J. F. P. Hudson: Knotted tori *Topology* 2 (1963) 11-22.
- [11] V. F. R. Jones: Hecke Algebra representations of braid groups and link *Ann. of Math.* 126, 335-388, 1987.
- [12] L. H. Kauffman: State models and the Jones polynomial *Topology* 26 (1987) 395-407.
- [13] L. H. Kauffman and H. Saleur: Free fermions and the Alexander-Conway polynomial *Comm. Math. Phys.* 141 (1991) 293-327.
- [14] L. H. Kauffman: Knots and physics, Second Edition. *World Scientific Publishing* 1994.
- [15] L. H. Kauffman: Talks at MSRI Meeting in January 1997, AMS Meeting at University of Maryland, College Park in March 1997, Isaac Newton Institute Lecture in November 1997, Knots in Hellas Meeting in Delphi, Greece in July 1998, APCTP-NANKAI Symposium on Yang-Baxter Systems, Non-Linear Models and Applications at Seoul, Korea in October 1998
- [16] L. H. Kauffman: Virtual knot theory, *European J. Combin.* 20 (1999) 663-690, math/9811028 [math.GT].
- [17] L. H. Kauffman: Introduction to virtual knot theory, *J. Knot Theory Ramifications* 21 (2012), no. 13, 1240007, 37 pp.
- [18] L. H. Kauffman: Rotational virtual knots and quantum link invariants. *J. Knot Theory Ramifications* 24 (2015), no. 13, 1541008, 46 pp.

- [19] L. H. Kauffman: Chern-Simons theory, Vassiliev invariants, loop quantum gravity and functional integration without integration. *Internat. J. Modern Phys. A* 30 (2015), no. 35, 1530067, 27 pp.
- [20] L. H. Kauffman and E. Ogasa: Local moves of knots and products of knots, *Volume three of Knots in Poland III, Banach Center Publications* 103 (2014) 159-209, arXiv: 1210.4667 [math.GT].
- [21] L. H. Kauffman and E. Ogasa: Local moves on knots and products of knots II, arXiv: 1406.5573[math.GT].
- [22] L. H. Kauffman and E. Ogasa: Brieskorn submanifolds, Local moves on knots, and knot products, *Journal of knot theory and its ramifications*, (to appear) arXiv: 1504.01229 [math.GT].
- [23] R. Kirby: The topology of 4-manifolds, *Lecture Notes in Math. (SpringerVerlag)* 1374 (1989).
- [24] R. Kirby and P. Melvin: The 3-manifold invariants of Witten and Reshetikhin-Turaev for $sl(2, \mathbb{C})$ *Inventiones mathematicae* 105 (1991) 473-545.
- [25] T. Kohno: Conformal field theory and topology. Translated from the 1998 Japanese original by the author. Translations of Mathematical Monographs, 210. Iwanami Series in Modern Mathematics. American Mathematical Society, Providence, RI, 2002. x+172 pp. ISBN: 0-8218-2130-X
- [26] T. D. Lee and C. N. Yang; Theory of Charged Vector Mesons Interacting with the Electromagnetic Field, *Phys. Rev.* 128 (885) 1962.
- [27] J. Levine: A classification of differentiable knots. *Annals of Math.* 82 (1965) 15-50.
- [28] J. Levine and K.E. Orr: A survey of applications of surgery to knot and link theory *Surveys on surgery theory: surveys presented in honor of C.T.C. Wall Vol. 1, 345-364, Ann. of Math. Stud., 145, Princeton Univ. Press, Princeton, NJ, (2000).*
- [29] W. B. R. Lickorish: Invariants for 3-manifolds from the combinatorics of the Jones polynomial *Pacific J. Math.* 149 (1991) 337-347.
- [30] W. B. R. Lickorish: Three-manifolds and the Temperley-Lieb algebra *Mathematische Annalen* 290 (1991) 657-670.
- [31] E. Ogasa: The intersection of spheres in a sphere and a new application of the Sato-Levine invariant, *Proceedings of the American Mathematical Society* 126 (1998).3109-3116, UTMS95-54.
- [32] E. Ogasa: Intersectional pairs of n -knots, local moves of n -knots and invariants of n -knots, *Math. Res. Lett.* 5 (1998) 577-582, Univ. of Tokyo preprint UTMS 95-50.
- [33] E. Ogasa: Supersymmetry, homology with twisted coefficients and n -dimensional knots, *International Journal of Modern Physics A* 21, (2006), pp.4185-4196, hep-th/0311136.
- [34] E. Ogasa: Make your Boy surface, arXiv:1303.6448 math.GT
- [35] E. Ogasa: Introduction to high dimensional knots, arXiv:1304.6053 [math.GT].
- [36] N. Reshetikhin and V. G. Turaev: Invariants of 3-manifolds via link polynomials and quantum groups, *Inventiones mathematicae* 103 (1991) 547-597.
- [37] D. Rolfsen: Knots and links *Publish or Perish, Inc.* 1976.
- [38] C. P. Rourke: What is a welded link? *Intelligence of low dimensional topology 2006, Ser. Knots and Everything, 40, World Sci. Publ., Hackensack, NJ (2007)* 263-270.
- [39] L. H. Ryder: Quantum Field Theory, Cambridge University Press, the second edition 1996.
- [40] S. Satoh: Virtual knot presentation of ribbon torus-knots *J. Knot Theory Ramifications* 9 (2000) 531-542.
- [41] J. Schneider: Diagrammatic Theories of 1- and 2- Dimensional Knots, *PhD thesis, University of Illinois Chicago.* (2016). The readers may find this article in <https://www.lib.umich.edu/>.

- [42] Y. Takeda: Introduction to virtual surface-knot theory *J. Knot Theory Ramifications* 21 (2012) 1250131 6pp.
- [43] D. Thurston: Private communication between Bar-Nathan, Dancso, and D. Thurston written in [1, section 10.2] and [2, section 3.1.1].
- [44] E. Witten: Quantum field theory and the Jones polynomial *Comm. Math. Phys.* 121, 351-399, 1989.
- [45] E. Zeeman: Twisting spun knots, *Trans. Amer. Math. Soc.*, 115 (1965) 471-495.

Acknowledgment. Kauffman's work was supported by the Laboratory of Topology and Dynamics, Novosibirsk State University (contract no.14.Y26.31.0025 with the Ministry of Education and Science of the Russian Federation).

Louis H. Kauffman: Department of Mathematics, Statistics and Computer Science
851 South Morgan Street University of Illinois at Chicago Chicago, Illinois 60607-7045,
and
Department of Mechanics and Mathematics, Novosibirsk State University, Novosibirsk,
Russia kauffman@uic.edu

Eiji Ogasa: Computer Science, Meijigakuin University, Yokohama, Kanagawa, 244-8539,
Japan pqr100pqr100@yahoo.co.jp ogasa@mail1.meijigakuin.ac.jp

Jonathan Schneider: Department of Mathematics, College of DuPage, 425 Fawell Boulevard,
Glen Ellyn, Illinois, 60137, USA jschneider.math@gmail.com